

NASA CONTRACTOR REPORT

NASA CR-1374



NASA CR-1374

0060532



TECH LIBRARY KAFB, NM

LEON S. ...
...
KIRTLAND AIR FORCE BASE

A PROGRAM TO EVALUATE DYE LASERS AS HIGH POWER, PULSED, VISIBLE LIGHT SOURCES

by Michael Bass, Thomas Deutsch, and Marvin Weber

Prepared by
RAYTHEON COMPANY
Waltham, Mass.
for Electronics Research Center



NASA CR-1374

A PROGRAM TO EVALUATE DYE LASERS AS HIGH POWER,
PULSED, VISIBLE LIGHT SOURCES

By Michael Bass, Thomas Deutsch, and Marvin Weber

Distribution of this report is provided in the interest of
information exchange. Responsibility for the contents
resides in the author or organization that prepared it.

Issued by Originator as Report No. S-1112

Prepared under Contract No. NAS 12-635 by
RAYTHEON COMPANY
Waltham, Mass.

for Electronics Research Center

NATIONAL AERONAUTICS AND SPACE ADMINISTRATION

For sale by the Clearinghouse for Federal Scientific and Technical Information
Springfield, Virginia 22151 - CFSTI price \$3.00

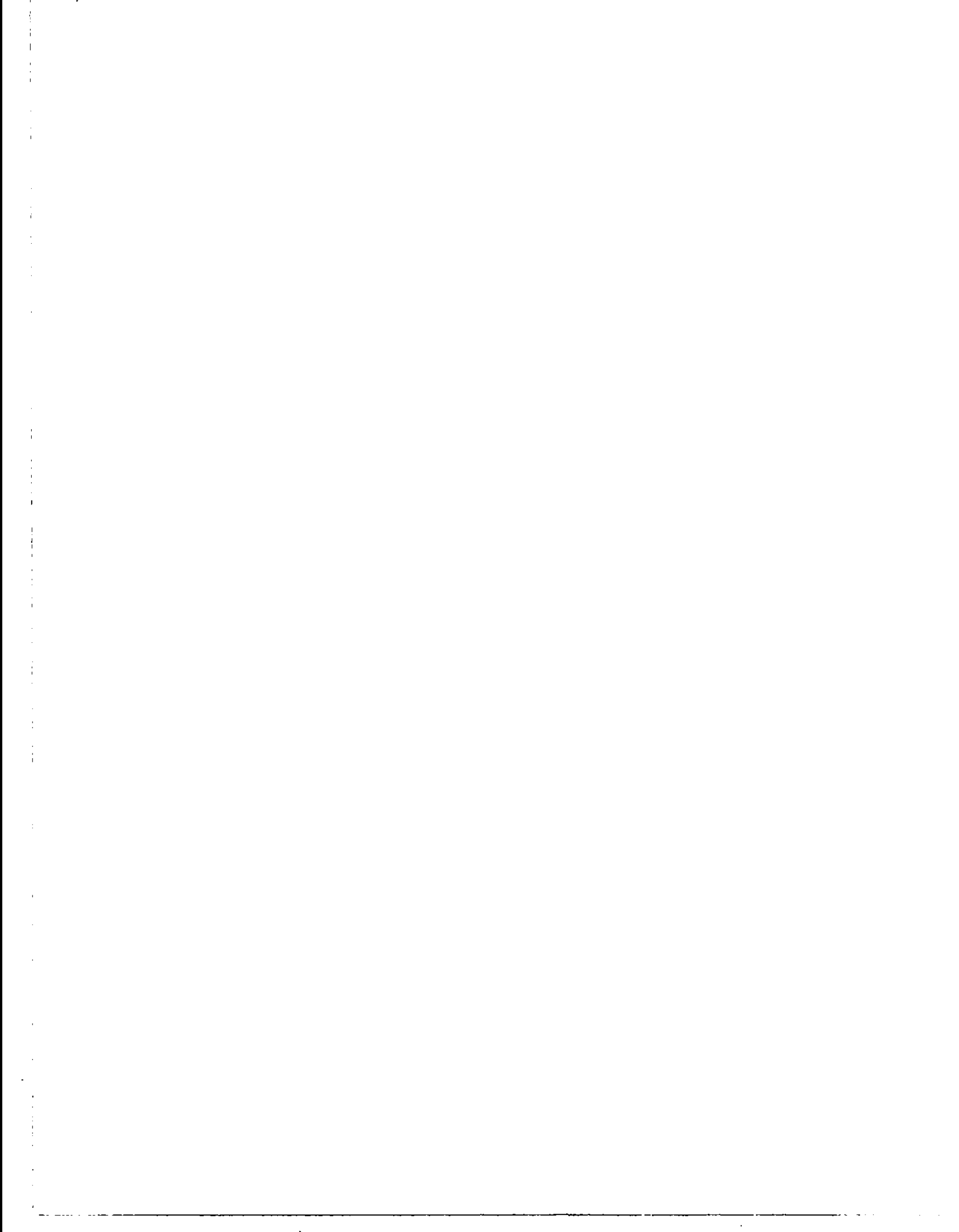


TABLE OF CONTENTS

	<u>Page</u>
I. SUMMARY	1
II. INTRODUCTION	4
III. INVESTIGATION OF DYE LASERS	9
A. Frequency- and Time-Dependent Gain Characteristics of Dye Lasers	9
1. Introduction	9
2. Theory	10
a. Gain-Frequency Dependence	12
b. Gain-Time Dependence	14
3. Gain Calculations with no Intersystem Crossing	18
a. Rhodamine 6G	18
b. 7-Hydroxycoumarin	29
4. Gain Calculations Where Intersystem Crossing Is Important	32
a. Anthracene	33
b. Rhodamine B	36
5. Flashlamp Pumping Criterion	44
6. Concluding Remarks	48
B. Addition Experiments	50
IV. CONCLUSIONS	52
REFERENCES	53
Appendix A - Dye Lasers: The Threepenny Laser	55
Appendix B - Frequency- and Time-Dependent Gain Characteristics of Laser- and Flashlamp-Pumped Dye Solution Lasers	65

LIST OF ILLUSTRATIONS

<u>Number</u>	<u>Title</u>	<u>Page</u>
1	Absorption and Emission Spectra of a Dye Solution	4
2	Schematic Energy-Level Diagram of a Dye Molecule Showing the Transitions Relevant to Dye Laser Action	5
3	Methods of Dye Laser Excitation	7
4	Energy-Level Diagram for an Organic Dye Molecule and Transitions Relevant to Laser Action	11
5	Absorption and Fluorescence Spectra of 10^{-4} M Rhodamine 6G in Ethanol	19
6	Calculated Gain of Rhodamine 6G as a Function of Frequency for Various Fractional Populations n_S in the First Excited Singlet State	20
7	Calculated Lasing Frequency of Rhodamine 6G Plotted vs the Fraction n_S of Molecules in the First Excited Singlet State	21
8	Flashlamp Excitation Pulse $\gamma(t)$ and Calculated Fraction n_S of Rhodamine 6G Molecules in the First Excited State	23
9	Predicted Lasing Frequency and Observed Lasing Bands of Rhodamine 6G for Various Cavity Q's	24
10	Observed Time at Threshold for Rhodamine 6G Laser Action as a Function of Input Energy to the Flashlamp	25
11	Experimental Arrangement Used for Q-Switched Laser Studies	27
12	Output Spectrum of a Q-Switched Rhodamine 6G Laser Using the Experimental Arrangement in Fig. 14	28
13	Time at Threshold for Oscillation of Rhodamine 6G as a Function of Pumping Intensity $ \gamma _{\max}$, Where $\gamma(t)$ Is Given in Fig. 8.	30
14	Calculated Gain Curves for 10^{-3} M 7-hydroxycoumarin at Various Time During Pumping	31
15	Singlet Fluorescence Spectrum and Triplet-Triplet Absorption Spectrum for Anthracene	34
16	Calculated Times Variations of the First Excited Singlet and Triplet Level Populations of Anthracene for a Pumping Pulse $\gamma(t)$	35
17	Calculated Gain as a Function of Frequency for Anthracene at Various Times During the Pumping Pulse Shown in Fig. 16.	37

LIST OF ILLUSTRATIONS (Cont'd)

<u>Number</u>	<u>Title</u>	<u>Page</u>
18	Singlet Absorption and Fluorescence Spectra of 5×10^{-5} M Rhodamine B in Methanol and Triplet-Triplet Absorption Spectrum in Polymethylmethacrylate	39
19	Flashlamp Pumping Function $\gamma(t)$ and Calculated Excited Singlet and Triplet Level Populations n_S and n_T of Rhodamine B for Different Choices of Intersystem Crossing Parameter $\eta = k_{ST}\tau_S$	40
20	Calculated Gain Curves for Rhodamine B at Various Times During Flashlamp Pumping. Intersystem Crossing Parameter $\eta = 0.2$	41
21	Calculated Gain Curves for Rhodamine B at Various Times During Flashlamp Pumping. Intersystem Crossing Parameter $\eta = 0.1$	42
22	Calculated Gain Curves for Rhodamine B at Various Times During Flashlamp Pumping. Intersystem Crossing Parameter $\eta = 0.05$	43
23	$k_{ST}T_\ell(\omega)$ vs ω from Eq. 19 for Rhodamine B	46

I. SUMMARY

This report describes our experimental and theoretical efforts to understand dye laser operation. The approach used by McCumber¹ for treating phonon-terminated lasers was applied to investigate the gain properties of dye lasers and was extended to include effects arising from population buildup in the triplet-level system and associated triplet-triplet absorptive losses. The gain is expressed in terms of time-dependent excited-state populations and spectral emission and/or absorption functions. For a given optical-pump pulse, a computer program was used to solve rate equations for the populations up to threshold and to calculate therefrom the gain as a function of time and frequency. The gain varies with frequency over the broad fluorescence bands characteristic of dye molecules and with time until the threshold for laser action is reached. Experiments using rhodamine 6G verify the predicted dependence of the laser frequency and time of threshold on cavity Q and demonstrate laser frequency tuning by adjusting the opening time of an intracavity Q switch. No variation of laser frequency is expected for fluorescing molecules exhibiting large Stokes shifts; this is observed for 7-hydroxycoumarin. Computer calculations of the gain for anthracene and rhodamine B illustrate the dependence of gain properties on the rate of intersystem crossing and triplet-triplet absorption. An estimate of the rate of intersystem crossing for rhodamine B in methanol is obtained from a comparison of predicted and observed laser threshold conditions.

This theory is also used to show how to determine whether a particular flashlamp will be able to excite lasing in a particular dye. To date it has been common practice to impose on dye laser flashlamps the condition that in order to achieve lasing they must reach their maximum intensity in a time, T , less than the time, τ_{ℓ} , when the net gain becomes negative due to the growth of triplet-triplet absorption. We show that this condition is neither necessary nor sufficient for success in exciting lasing. Instead, the important quantity is shown to be the net integrated flashlamp intensity up to the moment when the gain is maximum.

Experimental evidence is presented in support of our theoretical conclusions. Laser frequency tuning by each of the three methods mentioned above is demonstrated. In addition we report lasing four dyes with a simple, easy-to-assemble linear flashlamp pump system.

II. INTRODUCTION

The active medium in dye laser is a solution of an organic dye in either a liquid or a plastic host.* The first dye laser was demonstrated by Sorokin and Lankard² in March 1966; they used a Q-switched ruby laser to excite a solution of chloroaluminum phthalocyanine in ethanol. Dye lasers studied since have been both laser and flashlamp pumped and have emitted at wavelengths from ~ 0.45 to $\sim 1.06\mu$.

The general characteristics of the absorption and emission spectra of dye solutions are shown in Fig. 1. These curves and their relationship to dye laser action can be qualitatively understood by examination of Fig. 2, which shows schematically the energy levels of a dye molecule in solution. Each level represents a particular electronic, vibrational, and rotational state of the molecule. Since the electronic contribution to the energy is by far the largest, these levels are grouped together according to their electronic state and by their net electronic spin, either 0 or 1, into groups of singlets or triplets, respectively. Since it is impossible to represent the exact molecular configuration, we shall arbitrarily define the distance from the solid vertical line (on the left in Fig. 2) to represent the molecular configuration corresponding to the group of levels. Since electronic excitation takes place much faster than the molecule's configuration can change, absorption and emission are shown vertically in Fig. 2. After absorption from S_0 to S_1 , the molecule relaxes nonradiatively to the lower levels of S_1 whence it can emit a photon of less energy than the one absorbed. This accounts for the Stokes shift of fluorescence from absorption in dye solutions.

Examining Figs. 1 and 2, we see that the dye solution can emit where there is little or no absorption. The energy level scheme for S-S fluorescence is like that of a four-level laser and suggests the possibility of achieving laser action in these solutions.

*Much of this introductory material may also be found in Appendix A.

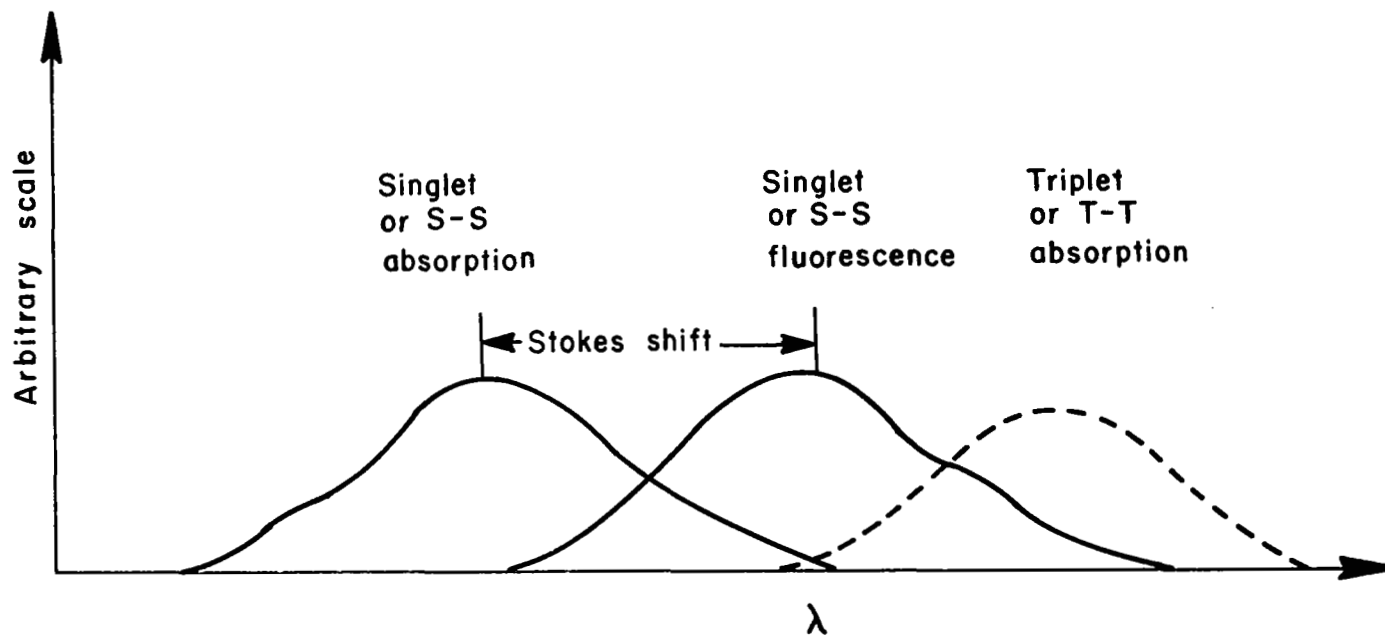


Fig. 1 Absorption and Emission Spectra of a Dye Solution

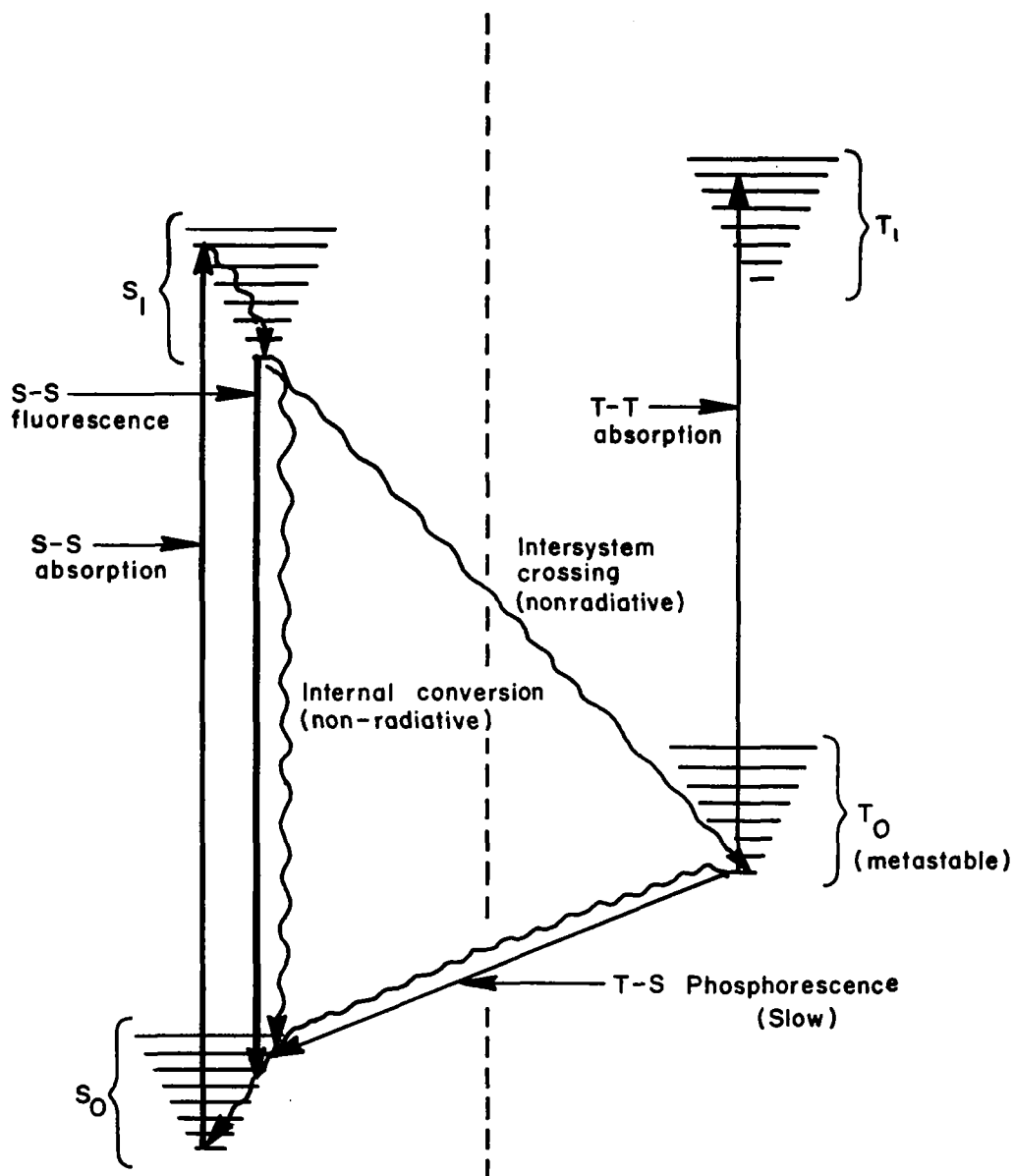


Fig. 2 Schematic Energy-Level Diagram of a Dye Molecule Showing the Transitions Relevant to Dye Laser Action

The achievement of lasing is hindered by two facts: the radiative lifetimes of most dye solutions are short (in general $\sim 5\text{nsec}$), and inter-system crossing to T_1 and internal conversion to S_0 are nonradiative loss mechanisms. In addition, T-T absorption may be in the same wavelength range as S-S fluorescence. This may cause a potential dye laser to not lase at all or to self-terminate due to the growth of T-T absorption. To achieve dye lasing it is, therefore, necessary to excite a sufficient population into S_1 before either the T-T absorption becomes large or the excited population decays away. For this reason a pump source must be energetic and fast: thus the first dye laser pumps were other laser beams (Fig. 3a). Since laser-pumped lasers are not very practical, flashlamps that could produce flashes of light with energies of ~ 10 to $\sim 100\text{J}$, with risetimes (time to the peak of the pulse) of $\sim 500\text{nsec}$ were developed. Sorokin et al.³ used an annular lamp, shown schematically in Fig. 3b, and a disc-shaped capacitor to achieve the desired flashlamp pulse. Schäfer et al.⁴ have also obtained laser action by exciting certain dye solutions with a commercial linear flashlamp, as shown in Fig. 3c.

In addition to those listed in Table I, there are dye lasers available to fill in almost the entire spectral range from 0.45 to $1.06\mu\text{m}$. The lasing wavelengths of most dye lasers can be tuned over very wide ranges (upwards of 200\AA) by varying the dye solvent,² varying the dye concentration,^{2, 5} adjusting the cavity Q ,⁶ and by Q-switching the dye laser.⁷ Soffer and McFarland⁸ have demonstrated that by using a diffraction grating as one of the cavity mirrors, one can narrow the lasing spectrum of a dye to less than 1\AA and select the laser wavelength without sacrificing much of the output energy.

The main body of this report (Sec. III) is composed of a paper on dye lasers which was originally prepared for publication in a scientific journal. As such it contains its own introductory segment and concluding remarks. For the sake of clarity and brevity neither of these items will be repeated elsewhere in this report. However, the reader might find it useful to read Appendix B before reading Sec. III since this appendix presents in a simplified form some of the salient points of our theory.

The second part of the next section contains additional descriptions of our experiments.

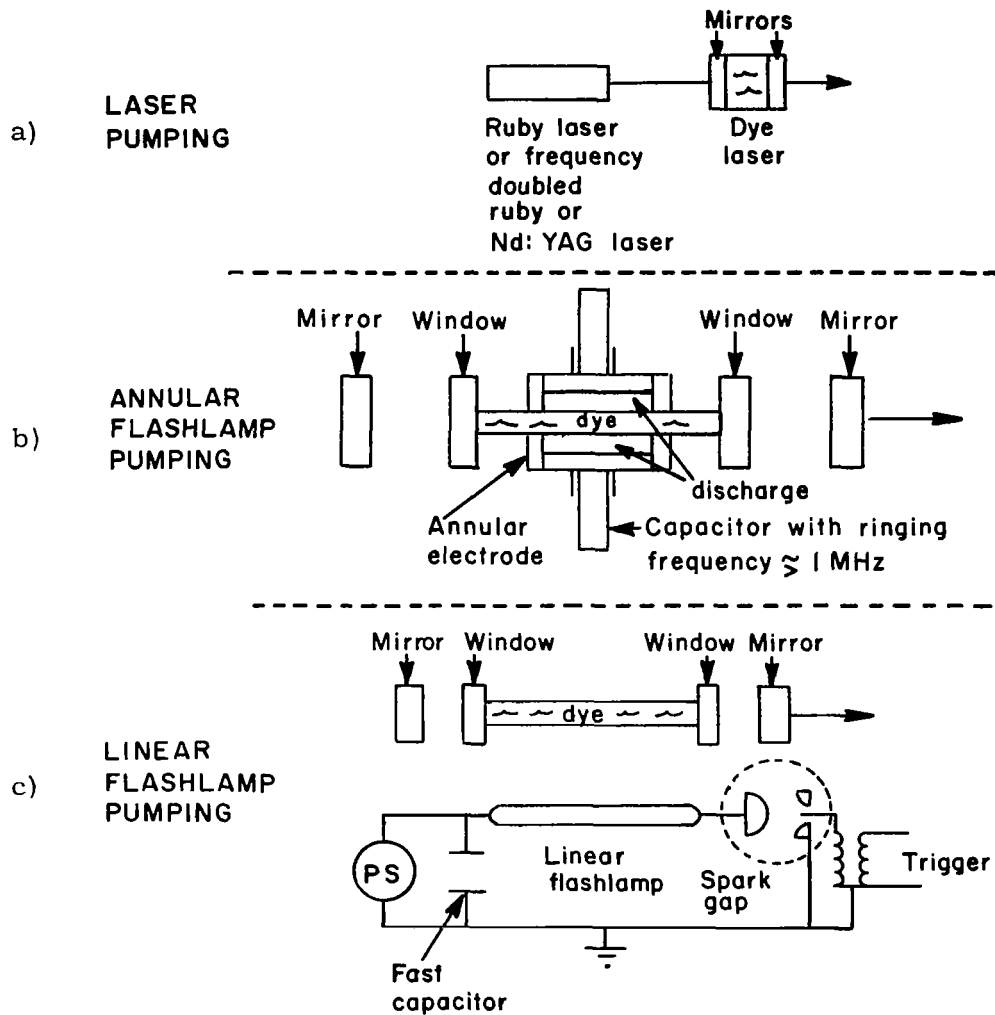


Fig. 3 Methods of Dye Laser Excitation

TABLE I
REPRESENTATIVE DYE LASERS

<u>Dye</u>	<u>Solvent</u> ^(a)	<u>Pumping Scheme</u> ^(b)	<u>Stability of Dye Solution</u>	<u>Lasing Wavelength (Å) and Color</u> ^(c)
7 hydroxycoumarin	water (buffered to pH =9)	AFPL	not stable	~ 4588, blue
7 diethylamino-4 methylcoumarin	ethanol	AFPL	stable	~ 4590, blue
fluorescein-Na salt	ethanol	LPL, AFPL	stable	~ 5370, green
rhodamine 6G	ethanol	LPL, AFPL, LFPL	stable	~ 5800, yellow
rhodamine B	ethanol	LPL, AFPL, LFPL	stable	~ 6100, red
pyronin B	methanol	AFPL	---	~ 6230, red
cryptocyanine	glycerol	LPL	not stable	~ 7300, deep red
DTTC iodide ^(d)	DMSO	LPL	not stable	~ 8000, near I. R.
Dye 11 ^(e)	acetone	LPL	---	~10,000, I. R.

(a) There may be several possible solvents.

(b) LPL = Laser pumped lasing
AFPL = Annular flashlamp pumped lasing
LFPL = Linear flashlamp pumped lasing

(c) When flashlamp pumped lasing has been achieved the wavelength and color given are for this type of excitation. Also note that the particular wavelength can be adjusted by $\pm \sim 150\text{Å}$ by adjustment of cavity Q and solution concentration.

(d) 3, 3'-diethylthiatriccyanine iodide

(e) 1, 1'-diethyl 4, 4'-quinotricarboyanine iodide, Y. Miyzoe and M. Maeda, Appl. Phys. Lett. 12, 206 (1968).

III. INVESTIGATION OF DYE LASERS

A. Frequency- and Time-Dependent Gain Characteristics of Dye Lasers

1. Introduction

During the past two years, pulsed laser action at visible and near-infrared wavelengths has been obtained from a large number of optically pumped organic dye molecules.⁹ In this paper, the frequency- and time-dependent gain characteristics of media containing dye molecules are examined theoretically and experimentally. The approach used is one originally developed by McCumber¹ to treat the frequency-dependent gain properties of phonon-terminated lasers. The gain is expressed in terms of calculated time-varying excited-state populations and measured spectral emission and/or absorption functions. The results show explicitly the manner in which the gain varies with frequency over the broad fluorescence spectrum of the dye and with time up to the moment the threshold for oscillation is reached. The dependence of these properties on the rate of optical pumping and on the modes and rates of decay of the excited state populations is also shown.

Gain calculations made using the above approach were applied recently to explain the observed dependence of lasing frequency on cavity Q and the different lasing frequencies reported for flashlamp vs laser pumping.¹⁰ The temperature dependence of the lasing frequency inherent in the theory has also been reported.¹¹ More extensive gain calculations, which illustrate the dependence of the gain on pump rate, cavity losses, and fluorescence spectrum, are presented herein. Predicted gain properties are confirmed by experiments using rhodamine 6G and 7-hydroxycoumarin. Also, a new technique predicted earlier¹⁰ for frequency tuning by adjusting the opening time of an intracavity Q-switch is demonstrated.

The relaxation of many optically excited dye molecules includes significant decay to the metastable triplet-level system. This transfer can be detrimental to laser action because (1) it reduces the number of molecules in the singlet system and hence the maximum gain possible,

and (2) it leads to additional losses if the triplet-triplet absorption spectrum overlaps the fluorescence spectrum. The gain expressions and rate equations have therefore been extended to include the effects of the triplet-level system. Quantitative gain calculations are frequently hampered, however, because the rates of intersystem crossing and the triplet-triplet spectra for molecules of interest are not known. The gain properties of anthracene and rhodamine B are computed to illustrate the time evolution of the gain and the effects of the triplet population buildup. Since the rate of intersystem crossing for rhodamine B was not known, calculations were made using a range of rate constants. It is shown that, by comparing the measured laser frequency and time of threshold with various predicted values, estimates of the intersystem crossing rate and the importance of the triplet-triplet losses can be obtained.

In a final section requirements for achieving laser action using flashlamp pumping are analyzed. Because of the continual buildup of triplet population, it is important that the pumping rate be sufficient to reach threshold gain before triplet losses become dominant. The required pumping conditions are dependent, in a complicated way, upon characteristics of both the flashlamp and the dye. Approximate expressions are derived which illustrate these relationships. The potential for lasing a particular dye-flashlamp combination can be more properly evaluated, however, using calculations of the frequency- and time- dependent gain characteristics as described in this paper.

2. Theory

The energy levels and transitions for organic dye molecules¹² of importance for laser operation are summarized in Fig. 4. Dye laser action has been obtained by optical pumping using short-pulse ($\sim 10^{-6}$ sec) flashlamp or Q-switched laser radiation. Molecules are excited into vibrational-rotational levels of S_1 or higher electronic singlet states and quickly decay nonradiatively to the lower levels of the S_1 manifold ($\sim 10^{-11} - 10^{-12}$ sec). From S_1 , molecules relax (1) to the singlet ground state radiatively by fluorescence and nonradiatively by internal conversion and (2) to the triplet level system by intersystem crossing,¹³ the total characteristic decay time being $\sim 10^{-8} - 10^{-9}$ sec. When the lowest triplet state is well below S_1 , it is usually metastable with a lifetime $> 10^{-4}$ sec. Relaxation from T_1 occurs by phosphorescence or by nonradiative decay if quenching impurities are present in the solution.

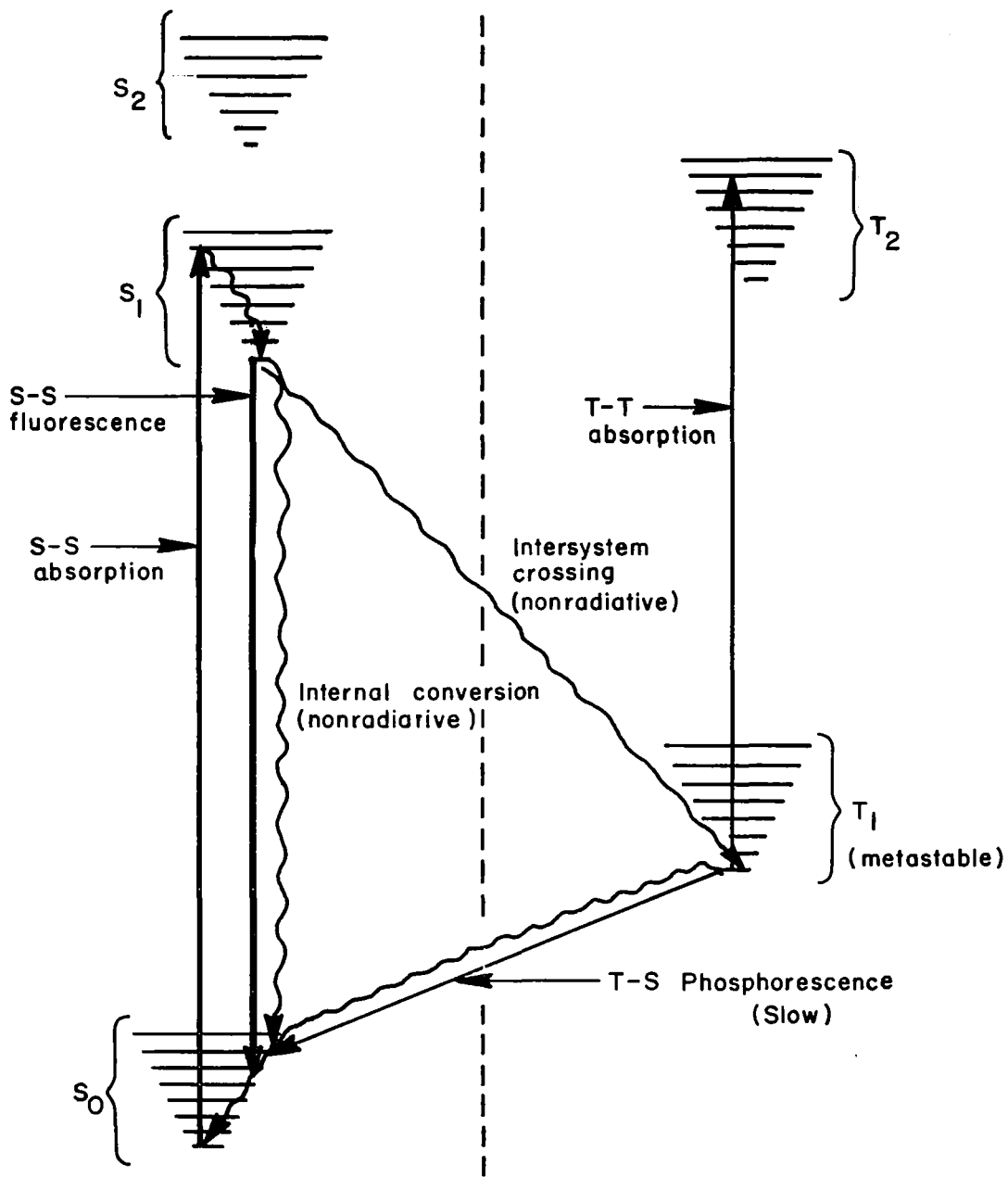


Fig. 4 Schematic Energy-Level Diagram of a Dye Molecule Showing the Transitions Relevant to Dye Laser Action

a. Gain-Frequency Dependence

Laser emission arises from transitions between the lower levels of S_1 and high-lying vibrational levels of the ground state. The gain per unit length for photons of angular frequency ω with wavevector and polarization indices (\underline{k}, λ) is

$$G(\omega, \underline{k}, \lambda) = e(\omega, \underline{k}, \lambda) - a(\omega, \underline{k}, \lambda), \quad (1)$$

where $a(\omega, \underline{k}, \lambda)$ is the absorption coefficient of the laser medium and $e(\omega, \underline{k}, \lambda)$ is the corresponding stimulated emission coefficient. During intense optical pumping, a significant molecular population may accumulate in the lowest excited singlet and triplet states S_1 and T_1 . Thus in addition to absorptive losses associated with transitions from the ground state, other spin-allowed transitions $S_1 \rightarrow S$ and $T_1 \rightarrow T$ may be important. In terms of the total absorption cross-sections σ_i^a for electronic state i ,

$$a(\omega, \underline{k}, \lambda) = N_{S_0} \sigma_{S_0}^a(\omega, \underline{k}, \lambda) + N_{S_1} \sigma_{S_1}^a(\omega, \underline{k}, \lambda) + N_{T_1} \sigma_{T_1}^a(\omega, \underline{k}, \lambda), \quad (2)$$

where N_i is the number of molecules per unit volume in the i^{th} set of levels. The population within each set of vibrational levels for a given electronic state is assumed to attain a Boltzmann thermal equilibrium distribution characteristic of the host temperature in a time short compared to the rates of optical pumping and decay from S_1 . This is generally a good approximation, although the use of intense light pulses from Q-switched lasers can result in "hole-burning" and a non-Boltzmann population distribution in S_0 .¹⁴⁻¹⁷ Instances in which the above approximation may not be valid will be discussed elsewhere.

McCumber has shown¹ that the absorption and emission cross-sections for broadband transitions are related by

$$\frac{\sigma^a(\omega)}{\sigma^e(\omega)} = \exp[\hbar(\omega - \mu)/kT], \quad (3)$$

where $\hbar\mu$ is a temperature-dependent excitation potential given by the net free energy required to excite one molecule while maintaining the

lattice temperature T . Many dye molecules of interest have approximately mirror-image absorption and emission spectra; for these cases μ can be taken to be the frequency of the 0-0 transition between the lowest vibrational levels of S_0 and S_1 . Using Eqs. (1-3) and dropping the wavevector-polarization indices, the gain can be written as

$$G(\omega) = \{N_{S_1} \exp [\hbar(\mu - \omega)/kT] - N_{S_0}\} \sigma_{S_0}^a(\omega) - N_{S_1} \sigma_{S_1}^a(\omega) - N_{T_1} \sigma_{T_1}^a(\omega). \quad (4)$$

The absorption cross-section $\sigma_{S_0}^a$ at frequencies where the gain is large is usually very small and not readily measurable, thus Eq. (4) is more usefully expressed in terms of the emission cross-section. Using Eq. (3) and introducing a fluorescence function $f(\omega, \underline{k}, \lambda)$ defined by $\sigma_{S_1}^e(\omega) = f(\omega) [2\pi c/\omega n(\omega)]^2$, Eq. (4) becomes

$$G(\omega) = \{N_{S_1} - N_{S_0} \exp [-\hbar(\mu - \omega)/kT]\} \left(\frac{2\pi c}{\omega n(\omega)}\right)^2 f(\omega) - N_{S_1} \sigma_{S_1}^a(\omega) - N_{T_1} \sigma_{T_1}^a(\omega). \quad (5)$$

$n(\omega)$ is the index of refraction of the medium at frequency ω . The quantity $f(\omega)$ in Eq. (5) is the average intensity in photons per second per unit frequency interval per unit solid angle observed for each emitting molecule. It can be derived from the emission spectrum via

$$A(S_1 \rightarrow S_0) = \sum_{\lambda} \int_{4\pi} d\Omega_{\underline{k}, \lambda} \int_0^{\infty} \frac{f(\omega, \underline{k}, \lambda)}{2\pi} d\omega. \quad (6)$$

In Eq. (6) A is the spontaneous emission probability and is related to the excited state lifetime τ and quantum yield ϕ by $\tau A = \phi$. Since the spectrum of $f(\omega)$ depends upon the population distribution among the vibrational levels, it is a function of temperature T .¹¹ Therefore the $f(\omega)$ to be used in Eq. (5) must be determined for the temperature of interest.

Other terms can be added to Eq. (5), if needed, to account for dispersive losses associated with the laser cavity or the introduction of frequency-selective elements into the cavity.

Lasing in a broadband cavity will occur at the frequency of the highest peak of the $G(\omega)$ curve where $dG/d\omega = 0$. It is evident from Eqs. (4) and (5) that for a given temperature, the frequency at which the gain is a maximum, and hence the lasing frequency at threshold, is governed by a combination of the absorption and emission spectra and the population densities N_i . Because the latter changes during the optical pumping, the gain and the frequency of the gain peak are also time dependent.

b. Gain-Time Dependence

The level populations at any time after the initiation of pumping are obtained from solutions of the rate equations governing the excitation and relaxation processes. Since we shall be concerned with the gain only up to the threshold for oscillation, the photon field in the laser cavity and stimulated emission processes are omitted. (These will be treated in a subsequent paper.) Excitation is assumed to proceed via optical pumping into S_1 and/or higher excited singlet states followed by very rapid decay to a thermal equilibrium distribution among the lower vibrational levels of S_1 . Pumping wavelengths suitable for inducing emission from S_1 to S_0 or exciting molecules from S_1 or T_1 to higher excited states are assumed to be absent in the following calculations. Even if the latter wavelengths were present, the rates of decay back to S_1 or T_1 are generally very much faster than available flashlamp pumping rates and hence no significant net change in excited-state population occurs. The metastable T_1 level is considered to be located sufficiently far below S_1 that reverse intersystem transitions $T_1 \rightarrow S_1$ are negligible. Thus we treat a simple system consisting of three sets of energy levels: the lowest excited singlet (S) and triplet (T) states and the ground state (0).

The rate equations for the effective three-level system are:

$$\frac{dN_S}{dt} = - \frac{1}{\tau_S} N_S + P(t) N_0, \quad (7a)$$

$$\frac{dN_T}{dt} = - \frac{1}{\tau_T} N_T + k_{ST} N_S, \quad (7b)$$

$$\frac{dN_0}{dt} = - P(t) N_0 + \left(\frac{1}{\tau_S} - k_{ST} \right) N_S + \frac{1}{\tau_T} N_T, \quad (7c)$$

where τ_S and τ_T are the singlet and triplet state lifetimes, $P(t)$ is the optical pumping rate, and k_{ST} is the rate of intersystem crossing $S \rightarrow T$. The calculations can be scaled conveniently by introducing the following dimensionless quantities:

$$\begin{aligned} n_i &= N_i/N \\ x &= t/\tau_S \\ \gamma &= \tau_S P \\ \rho &= \tau_S/\tau_T \\ \eta &= \tau_S k_{ST} \end{aligned} \quad (8)$$

For a closed system and in the absence of photochemical processes, the total molecular concentration $N = N_S + N_T + N_0 = \text{constant}$. Eq. (7) can thus be rewritten

$$\frac{dn_S}{dx} = - (1 + \gamma)n_S - \gamma n_T + \gamma, \quad (9a)$$

$$\frac{dn_T}{dx} = - \rho n_T + \eta n_S \quad (9b)$$

and the gain is given by

$$g(\omega) = \frac{G}{N} = (n_S - n_0 e^{-\Omega}) \left(\frac{2\pi c}{\omega n(\omega)} \right)^2 f(\omega) - n_T \sigma_T(\omega), \quad (10)$$

where

$$\Omega = \hbar (\mu - \omega)/kT \quad (11)$$

For a given pumping function $\gamma(x\tau_S)$, the simultaneous differential equations in Eq. (9) are solved on a IBM 7044 computer using a predictor-corrector method. γ is taken to be constant over an x interval which was typically ~ 0.01 of the pumping pulse duration. Starting from their thermal equilibrium at $x = 0$, the populations n_S and n_T at later times are calculated and inserted into the gain expression together with the measured spectral functions, temperature, and estimated μ ; the final computer readout is the gain G as a function of ω at selected times during the pumping.

The frequency of the peak of the gain curve $G(\omega)$ changes during pumping until threshold is reached. The lasing frequency is therefore dependent upon the losses or the Q of the laser cavity. For cavities and dyes having time-independent losses, the lasing frequency, if threshold gain is attained, will always be the same, independent of the time and intensity properties of the optical-pump pulse; only the period of pumping to achieve threshold will vary.¹⁰

This is not the case, however, when time-varying losses, such as those arising from excited singlet and triplet state absorption, are present. If the triplet level has a lifetime long compared to both the pumping pulse and τ_S , a significant triplet population buildup may occur. The transfer of molecules to a metastable triplet level is proportional to the rate of intersystem crossing k_{ST} and is an integrating process during the pumping. It affects the gain in two ways: (1) the total number of molecules in the singlet system and the associated maximum gain possible are reduced and (2), if the T-T absorption overlaps the fluorescence, there is a loss mechanism increasing with time. Both can be detrimental to laser action. Since flashlamp pulses are generally very much longer than the τ_S of dye molecules, the number of molecules in T_1 can become a sizable fraction of the total population. The triplet population buildup is comparatively less important when short-pulse laser excitation is used, but is not necessarily negligible.

Three limiting cases can be readily distinguished for calculating gain properties of dye lasers:

I. $k_{ST} = 0$.

The triplet population $N_T(t) = 0$ at all times and hence the above effects of the triplet level system are absent. The simplified rate equations for this case have been presented previously in connection with the treatment of flashlamp-versus laser-pumped dye lasers.²⁰

II. $k_{ST} \neq 0$, $\tau_T \gg \tau_S$, T-T absorption does not overlap fluorescence spectrum.

If the pump pulse has a duration $\lesssim \tau_S$ and a rate $P(t)|_{\max} < \tau_S^{-1}$, the total population transfer to the triplet system before threshold is attained will be small; the gain can therefore be calculated as in I. Flashlamp pulses, however, are generally much longer and a population transfer sufficient to affect the gain may occur. Under weak pumping conditions (i. e. , $P(t) \tau_S \ll 1$), $N_S(t) \approx N_0 P(t) \tau_S$ and the gain can be written

$$G(\omega) \approx N_0 [P(t) \tau_S - e^{-\Omega}] \left(\frac{2\pi c}{\omega n(\omega)} \right)^2 f(\omega). \quad (12)$$

From Eq. (7b), the triplet population at time t after pumping begins is

$$N_T(t) \approx k_{ST} \int_0^t N_S(t) dt. \quad (13)$$

Because of this transfer, the population in the singlet system is continually decreasing and

$$N_0(t) \approx N - N_T(t) \approx N - k_{ST} \int_0^t N_S(t) dt. \quad (14)$$

Thus if the decrease of $N_0(t)$ exceeds the increase of the $P(t) \tau_S$ term in Eq. (12), the gain may actually begin to diminish before the peak pumping intensity is reached.

III. $k_{ST} \neq 0$, $\tau_T \gg \tau_S$, T-T absorption overlaps fluorescence spectrum.

The gain in this case must be calculated using Eq. (4) or (5) and solutions of the coupled rate equations in Eq. (7).

Application of the above gain theory for a known pump function $P(t)$ requires, in case I, knowledge of the $S_0 - S_1$ absorption or emission spectra, fluorescence lifetime τ_S , and quantum yield ϕ . Cases II and III require, in addition, knowledge of the T-T absorption cross-section $\sigma_T(\omega)$, triplet lifetime τ_T , and rate of intersystem crossing k_{ST} .

3. Gain Calculations with no Intersystem Crossing

The preceding formalism is first applied to calculate the gain when the rate of intersystem crossing is small and can be neglected. Two dyes, rhodamine 6G and 7-hydroxycoumarin, which have high fluorescence quantum efficiencies and which approximate this limiting case, are treated. The calculations were performed by setting $\eta = 0$ in Eq. (9). Since in this case $n_T = 0$ at all times, having measured $f(\omega)$, one need know only $n_S(t)$ to determine the gain and possible lasing frequency.

a. Rhodamine 6G

We have found that a 10^{-4} M solution of rhodamine 6G in ethanol is very nearly an optimal concentration for obtaining reliable, low threshold, and reasonably energetic laser action; therefore this solution was selected for detailed experimental and theoretical analysis. The absorption and fluorescence spectra are shown in Fig. 5. The fluorescence function $f(\omega)$ was scaled using a measured lifetime $\tau_S = 7.4$ nsec and the reported quantum yield⁽¹¹⁾ $\phi = 0.84$. Plots of $G(\omega)$ for various values of n_S are given in Fig. 6. In Fig. 7 the peak of the gain curve, and hence the lasing frequency at threshold is plotted versus n_S . To determine whether a given excitation pulse is sufficient

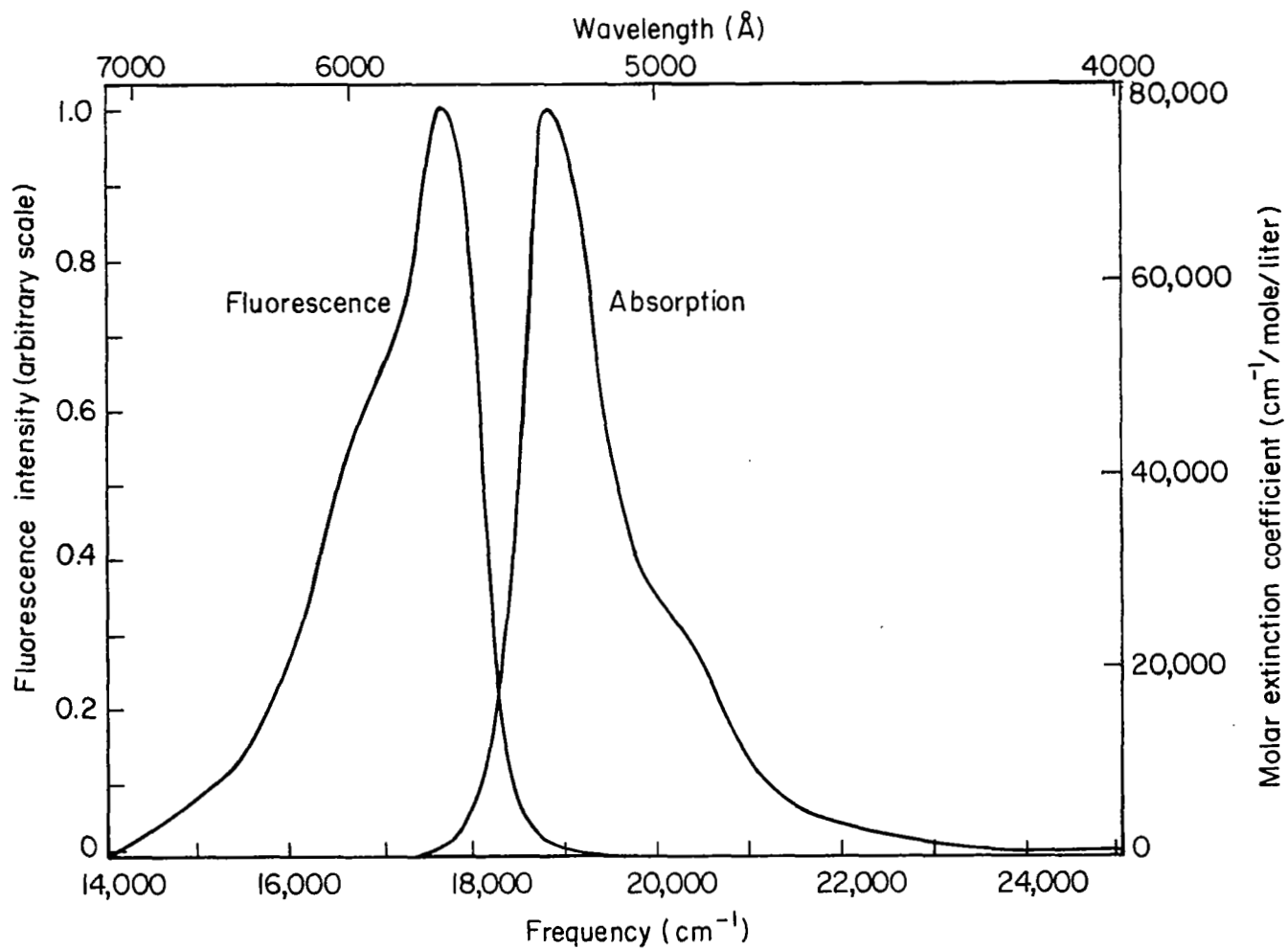


Fig. 5 Absorption and Fluorescence Spectra of 10^{-4} M Rhodamine 6G in Ethanol

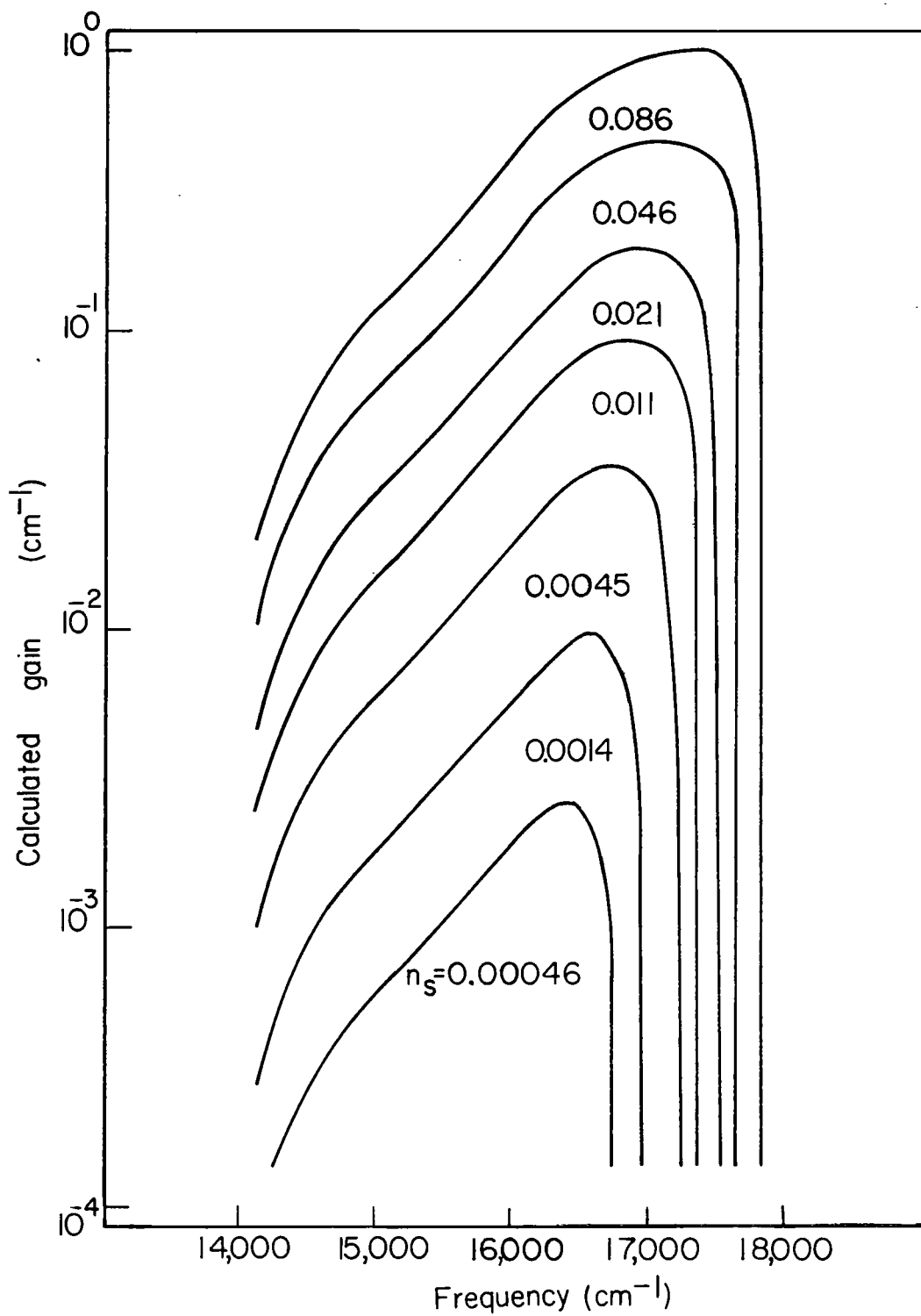


Fig. 6 Calculated Gain of Rhodamine 6G as a Function of Frequency for Various Fractional Populations n_s in the First Excited Singlet State

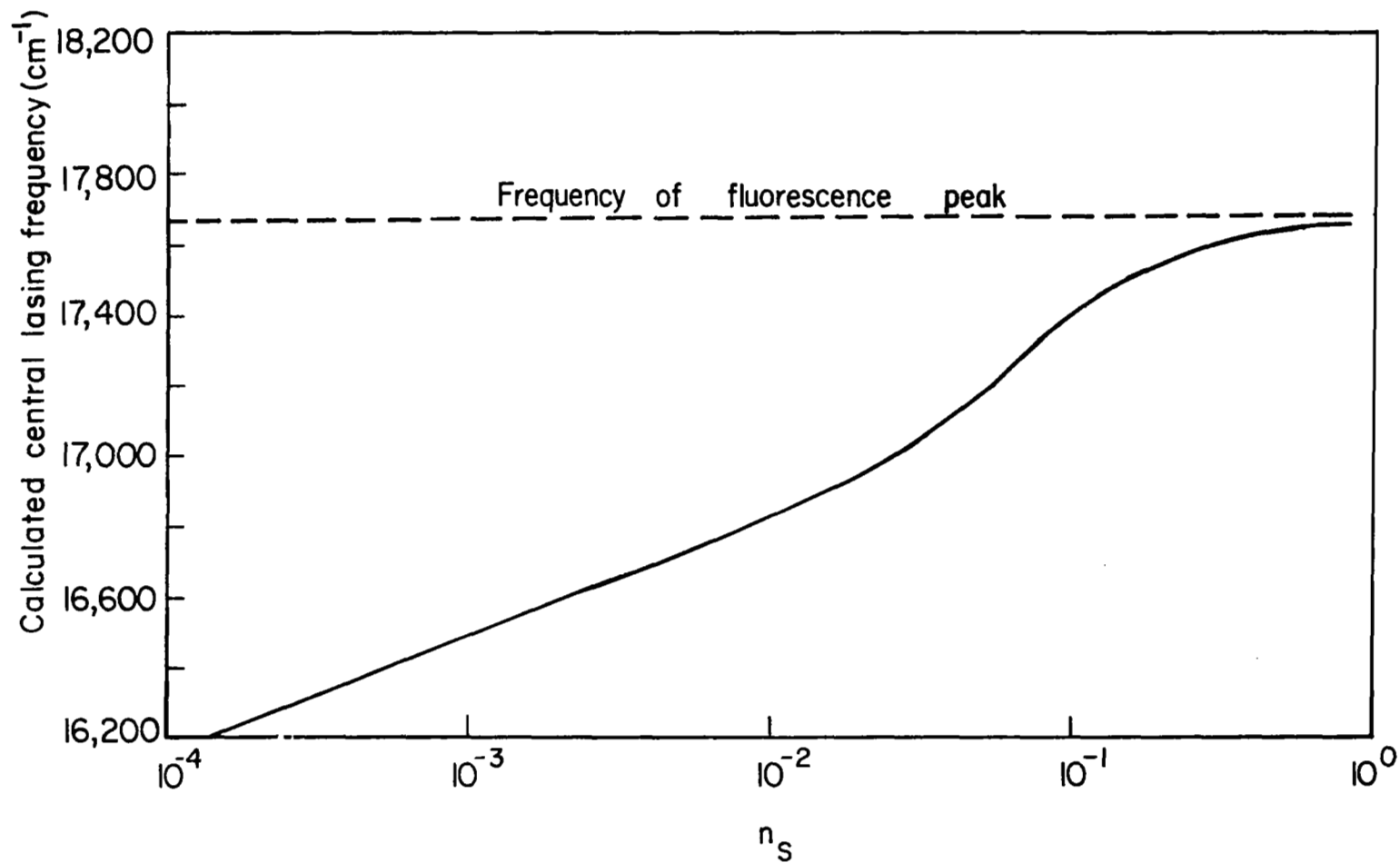


Fig. 7 Calculated Lasing Frequency of Rhodamine 6G Plotted vs the Fraction n_s of Molecules in the First Excited Singlet State

to achieve oscillation, one need only compute $n_S(t)$ and then select a cavity configuration having a threshold gain less than that corresponding to the largest value of n_S . Once the value of n_S required for threshold is known, the lasing frequency can be predicted from Fig. 4.

However, to calculate $n_S(t)$ from the rate equations, Eq. (7) or Eq. (9), one must accurately evaluate the pumping rate $P(t)$. Although the spectral properties of the pumping source and the dye absorption bands can be measured, the net absorption of pump light by the dye in a laser cavity is also determined by geometrical factors and scattering. Therefore, in practice, it may be difficult to determine the effective pumping rate with a high degree of accuracy. (See the discussion of this point in Ref. 10.)

A typical flashlamp pumping function $\gamma(t)$ is shown in Fig. 8. It was obtained from an annular flashlamp used in the experiments reported below. The lamp was energized by a 0.25 μ f oil-filled capacitor having a large self-inductance of ≈ 1600 nH; it typically dissipated about 50J in the discharge. All subsequent calculations for rhodamine 6G were performed using the pulse shape in Fig. 8. The $n_S(t)$ calculated for $\gamma_{\max} = 0.03$ is also included in Fig. 8. Note that in general when the flashlamp pulse duration is $\gg \tau_S$ and $k_{ST} = 0$, the population $n_S(t)$ simply tracks $\gamma(t)$.

As an example, consider a cavity composed of one 100%R broadband mirror and one 60%R mirror. Allowing $\sim 5\%$ additional loss due to absorption by unpumped molecules and scattering, the threshold gain required for lasing would be $\sim 3.2 \times 10^{-2} \text{ cm}^{-1}$. From Fig. 6, this corresponds to $n_S \sim 0.45 \times 10^{-2}$, and thus, from Fig. 8, lasing should begin at $t \approx 250$ nsec. The expected lasing frequency according to Fig. 7 is $16,700 \text{ cm}^{-1}$. These predictions are confirmed by the experimental results reported in Figs. 9 and 10; these results will be discussed in greater detail below.

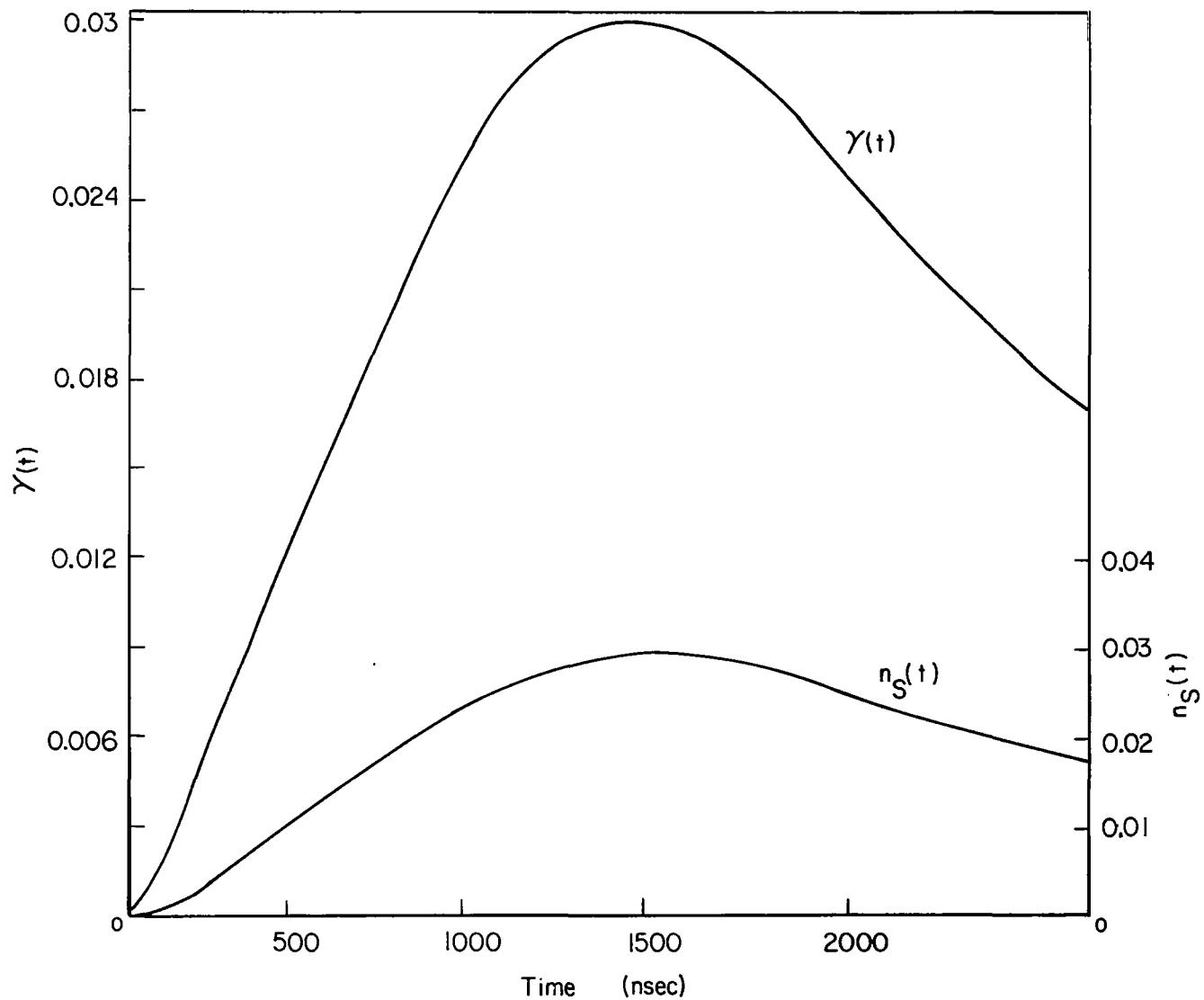


Fig. 8 Flashlamp Excitation Pulse $\gamma(t)$ and Calculated Fraction n_S of Rhodamine 6G Molecules in the First Excited State. Lifetime $\tau_S = 7.4$ nsec.

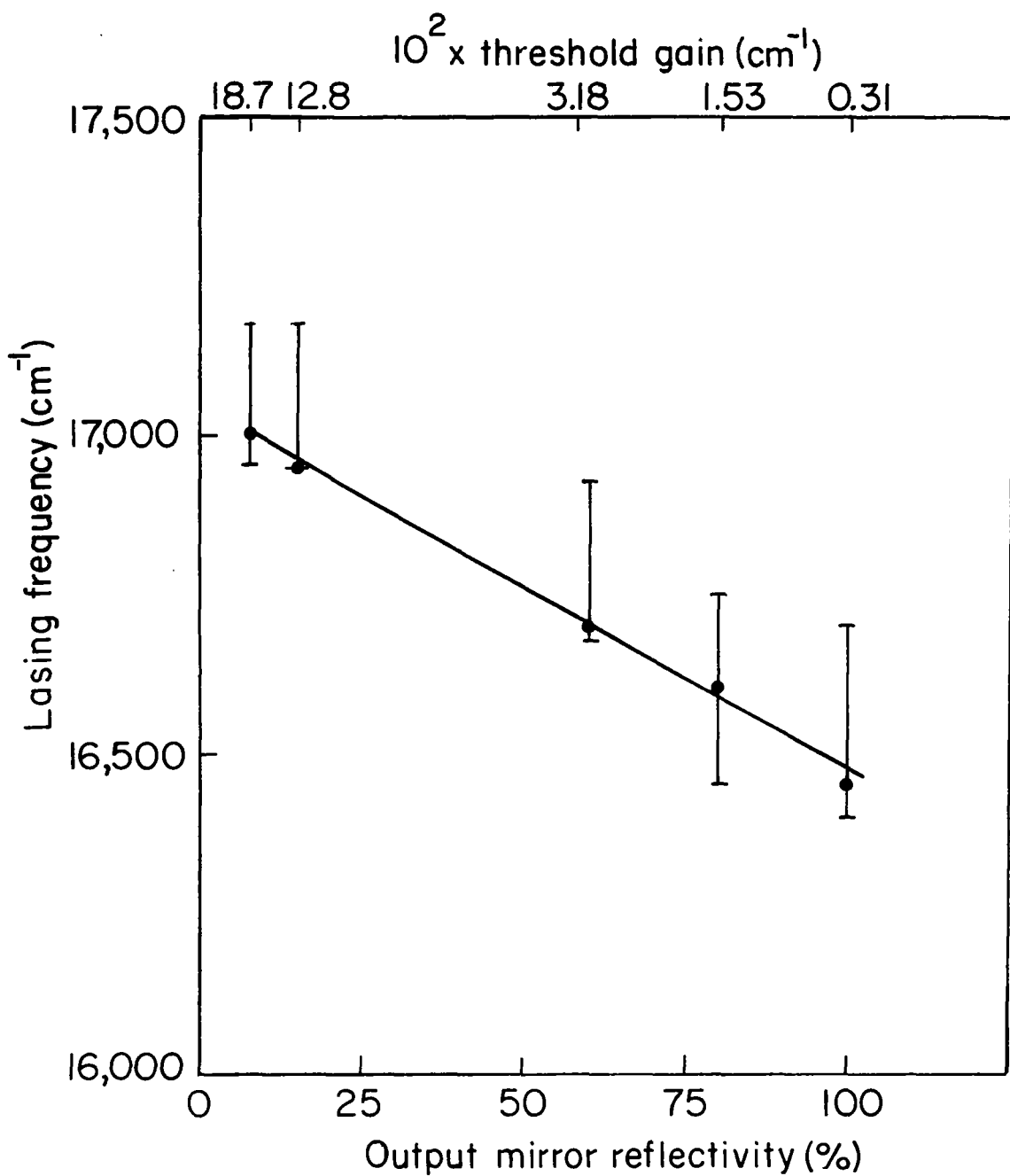


Fig. 9 Predicted Lasing Frequency (solid points) and Observed Lasing Bands (bars) of Rhodamine 6G for Various Cavity Q's. The cavity consisted of the indicated output mirror and a broadband 100 percent R mirror. The estimated threshold gain includes a 5 percent loss for the ~ 4 cm of unpumped solution.

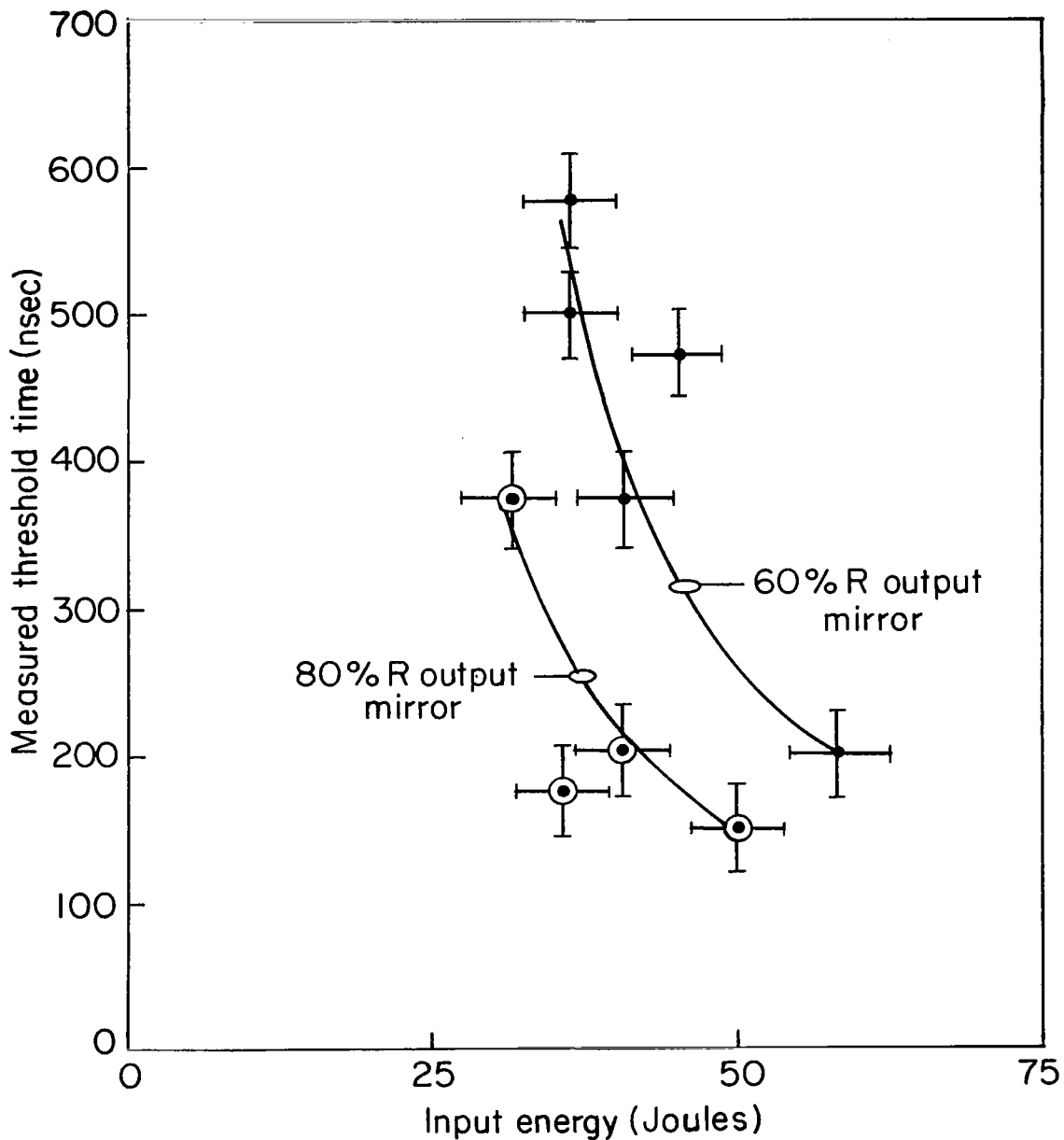


Fig. 10 Observed Time at Threshold for Rhodamine 6G Laser Action as a Function of Input Energy to the Flashlamp. A 100 percent R mirror and the indicated output mirror formed the laser cavity.

Two general comments are in order at this point. First, note that lasing threshold can be achieved when the inverted population is $\ll 0.5$ indicating that dye lasers are four-level lasing systems. Second, since the rate equations used do not contain terms accounting for stimulated emission from S_1 to S_0 , the population n_S can approach unity for strong pumping. This can occur, for example, when radiation from high-energy Q-switched lasers excites molecules to levels above the lowest level in S_1 , since there is no optical field present to stimulate $S_1 \rightarrow S_0$ transitions. If n_S does approach unity, the peak lasing gain must occur at the frequency where the fluorescent spectrum is most intense. Thus the curve in Fig. 7 approaches $17,700 \text{ cm}^{-1}$ tangentially as $n_S \rightarrow 1$.

Since n_S varies with time, the frequency at which the gain is maximum may also vary with time. In Ref. 7 a plot of this frequency for rhodamine B in methanol versus time, for a specific pump function, led to the prediction that the lasing wavelength could be varied by inserting a variable delay Q-switch in the optical cavity. Such an experiment was performed for rhodamine 6G using the apparatus sketched in Fig. 11; the results in Fig. 12 confirm the prediction. Because the lamp-capacitor combination used produced a pulse which peaked at $\tau_m \approx 900 \text{ nsec}$, spectra b and c in Fig. 12 were obtained when n_S was decreasing with time; thus the lasing wavelength should increase going from b to c. Unfortunately these results cannot be directly compared to the predicted time dependence of the lasing frequency obtained from Figs. 7 and 8 because the experimental pump function was not identical to that used in the calculations.

Both the magnitude of $g(\omega)$ and the wavelength at which it is maximum depend upon n_S and, through n_S , on the time lapse after initiating pumping. Therefore cavities having different Q's or threshold gain requirements will exhibit lasing at different frequencies. As seen from Figs. 6 and 7, low-Q cavities requiring high gain for oscillation will lase at higher frequencies (shorter

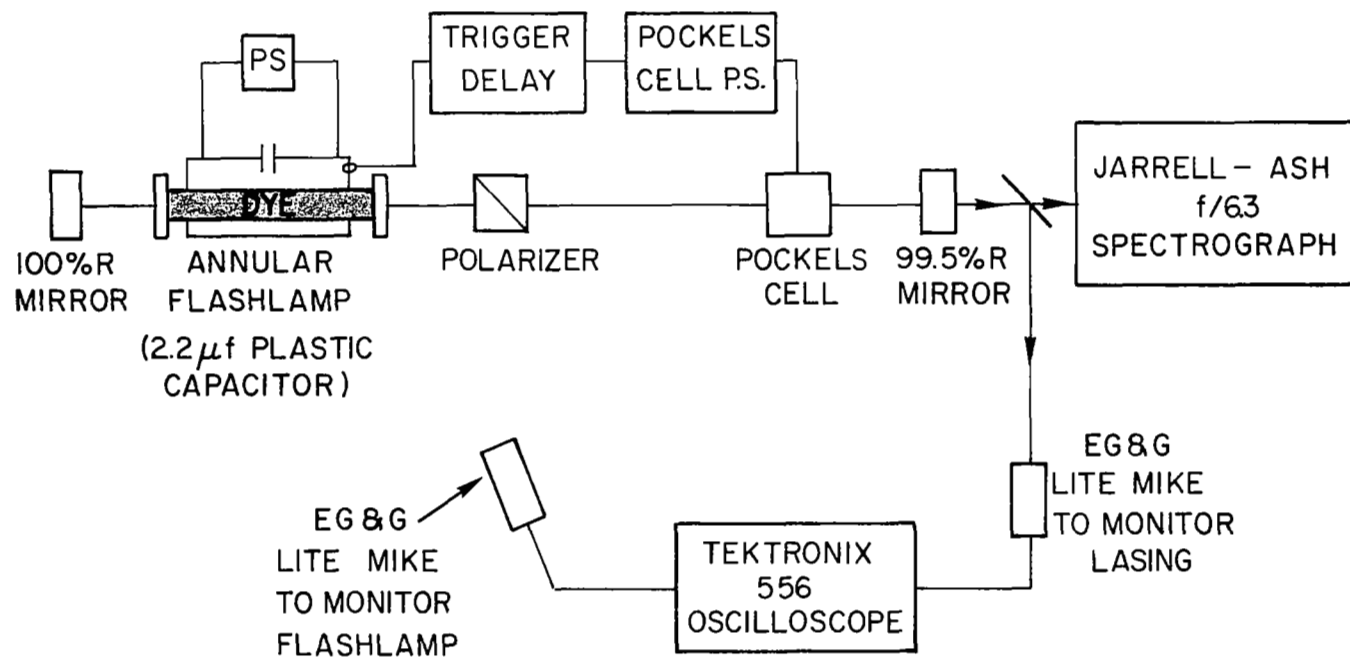


Fig. 11 Experimental Arrangement Used for Q-Switched Laser Studies

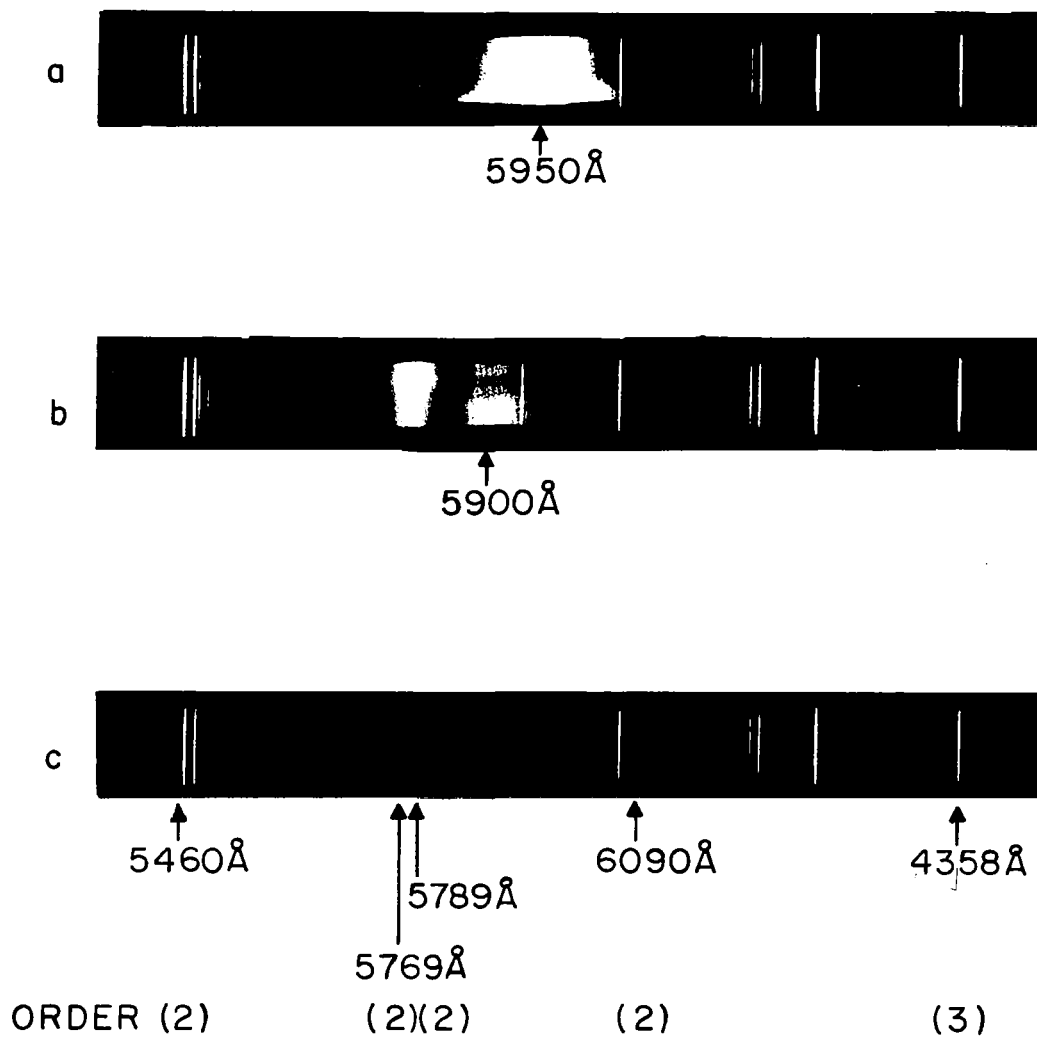


Fig. 12 Output Spectrum of a Q-Switched Rhodamine 6G Laser Using the Experimental Arrangement in Fig. 11.

- a) No voltage on Pockels cell
- b) Pockels cell opened at $1.04 \mu\text{sec}$ after initiation of pumping
- c) Pockels cell opened at $1.13 \mu\text{sec}$.

Since the Pockels cell does not always act as a perfect shutter, prepulsing can occur; the emission at $\approx 5780\text{\AA}$ in b) is due to lasing in the lower Q cavity formed when the Q-switch is still mainly closed.

wavelengths) than high- Q cavities. This is demonstrated explicitly in Fig. 9, where the experimentally observed lasing band for several choices of cavity mirrors is compared to the computed frequency for which $g(\omega) = g_{\text{threshold}}$.

Another facet of the dynamic behavior is that for a given pumping rate, threshold will be reached at different times for different cavity Q 's. This is shown in Fig. 13 where the computed time to achieve threshold gain is plotted versus the maximum value of the pump function γ for several choices of cavity mirrors. For certain low- Q cavities and weak pumping, lasing threshold is not reached. Fig. 10 shows the experimentally measured time to reach oscillation as a function of pump energy. These data exhibit the predicted behavior; however, since the gas pressure in the flash-lamp was varied to obtain firing with different voltages on the energy storage capacitor, the form of $\gamma(t)$ was not identical for each energy. Direct comparison of Figs. 13 and 10 is thus not possible.

b . 7-Hydroxycoumarin

Laser action from 7-hydroxycoumarin has been reported by Snavely and Peterson.¹⁸ Since the quantum yield is 0.99,^{18,19} intersystem crossing can be neglected. Gain calculations were made using the fluorescence spectrum measured for a $10^{-3}M$ solution of 7-hydroxycoumarin in water (pH = 9), $\tau_S = 5.5$ nsec, and $\phi = 0.99$. The results, together with the pump function used, are shown in Fig. 14. The Stokes shift for this solution is very large ($\approx 5000 \text{ cm}^{-1}$). In the approximation of mirror symmetry, $\hbar(\mu - \omega) \gtrsim 2500 \text{ cm}^{-1}$ and the exponential term in Eq. (5) is always small. The gain at room temperature and for frequencies less than or equal to that at the fluorescence peak can thus be written

$$g(\omega) \approx (n_S - 4 \times 10^{-6}) \left(\frac{2\pi c}{\omega n(\omega)} \right)^2 f(\omega) \quad . \quad (15)$$

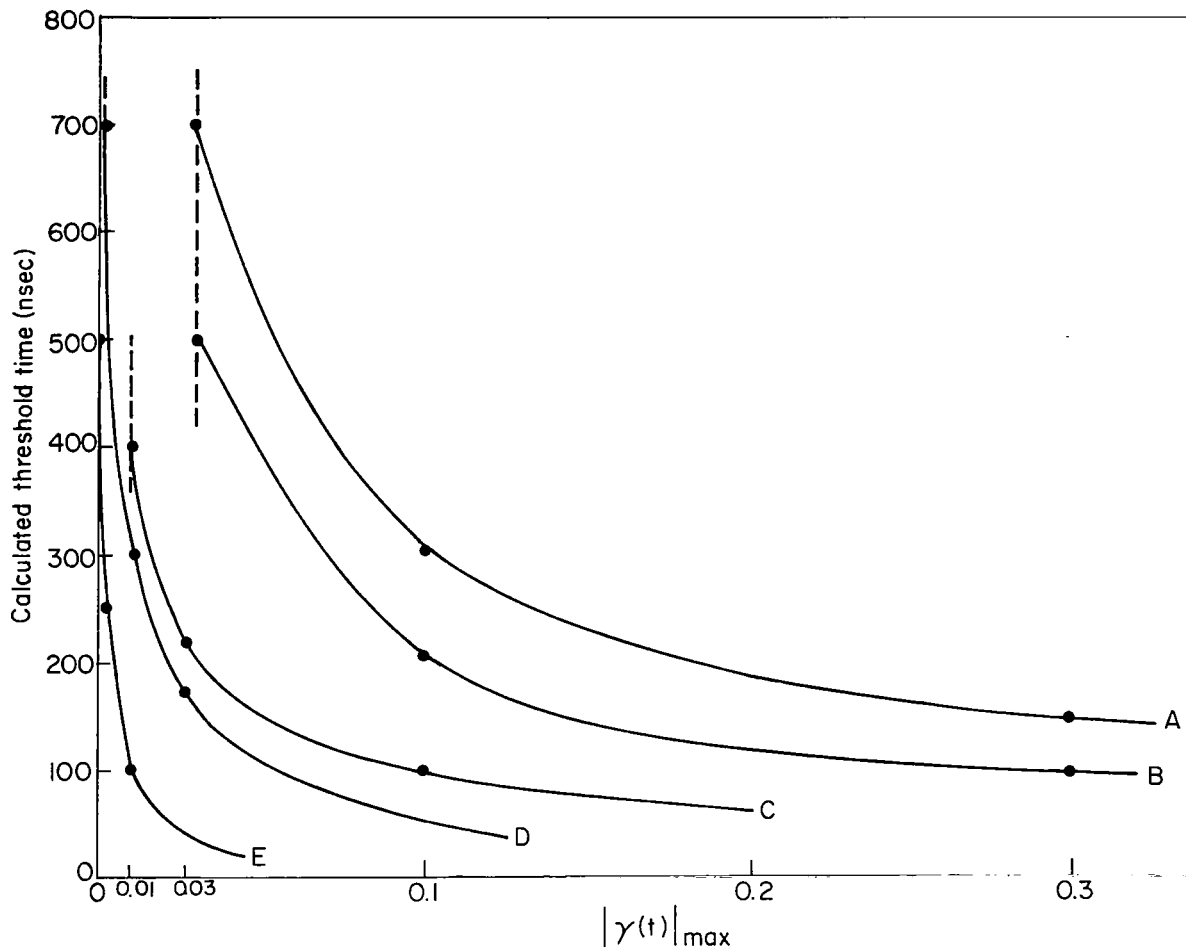


Fig. 13 Time at Threshold for Oscillation of Rhodamine 6G as a Function of Pumping Intensity $|\gamma|_{\max}$, where $\gamma(t)$ is given in Fig. 8. The cavities used had broadband mirrors and estimated gains required for threshold as follows:

- A - 100%R and 8%R mirrors, $G_{\text{threshold}} = 0.187 \text{ cm}^{-1}$
- B - 100%R and 14%R mirrors, $G_{\text{threshold}} = 0.128 \text{ cm}^{-1}$
- C - 100%R and 60%R mirrors, $G_{\text{threshold}} = 0.032 \text{ cm}^{-1}$
- D - 100%R and 80%R mirrors, $G_{\text{threshold}} = 0.015 \text{ cm}^{-1}$
- E - 100%R and 99.5%R mirrors, $G_{\text{threshold}} = 0.0031 \text{ cm}^{-1}$

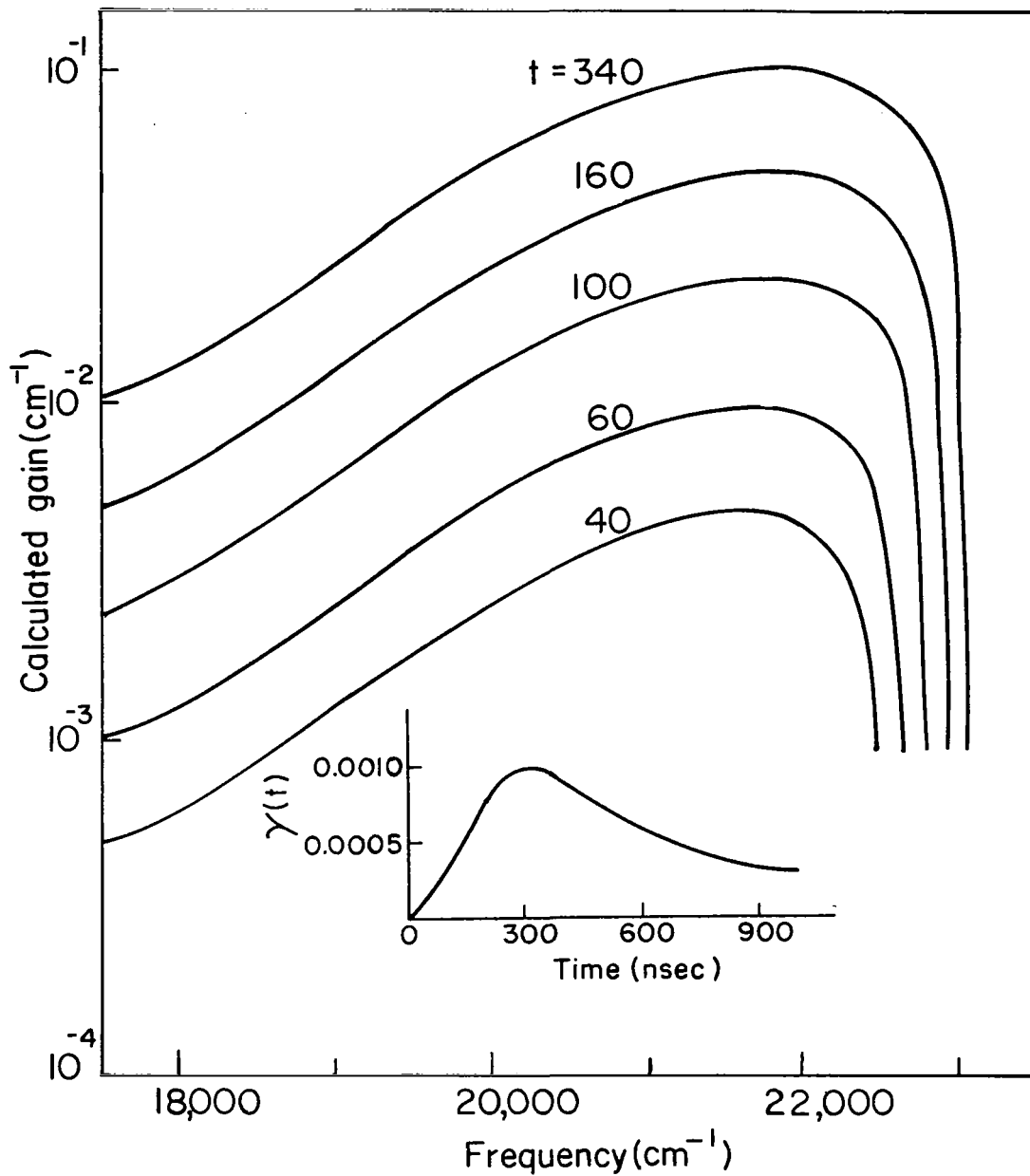


Fig. 14 Calculated Gain Curves for 10^{-3} M 7-Hydroxycoumarin at Various Times During Pumping. The time dependence and estimated intensity of the excitation pulse are shown in the insert.

Since for the flashlamp pulse considered, n_S is already $\approx 5 \times 10^{-5}$ at 40 nsec, the gain maximum and lasing will occur at the peak of the $f(\omega)$ fluorescence spectrum, $\omega = 21,800 \text{ cm}^{-1}$ (4590 \AA). There should be no change in frequency of $g(\omega) |_{\text{max}}$ and, except for the highest Q cavities, there should be no dependence of lasing wavelength on cavity Q (see Fig. 14). This is indeed observed. Using an annular flashlamp and cavities composed of one 100%R broadband mirror and either a 98%, 79%, or 49%R broadband mirror for output coupling, the measured central lasing wavelength was $(4588 \pm 5) \text{ \AA}$.

The behavior exhibited for 7-hydroxycoumarin may be generalized to other dyes. Whenever there is very little overlap of the fluorescence spectrum and the singlet or triplet absorption spectra, the lasing frequency will be independent of Q in a broadband cavity. This property can be utilized to check on the presence of T-T absorption in dyes with large Stokes shifts. The above results for 7-hydroxycoumarin support the notion that triplet absorption is unimportant for this dye.

4. Gain Calculations Where Intersystem Crossing Is Important

Analysis of the effects of population transfer to the triplet level system on laser gain and thresholds is frequently hampered because the rate of intersystem crossing and the T-T absorption spectrum for the molecule and solvent of interest are not known. Although the total nonradiative decay from S_1 can be readily determined from measurements of the fluorescence lifetime and quantum yield, the relative contributions of internal conversion and intersystem crossing¹³ remain to be established. Two examples are treated in this section. In the first case, anthracene, the T-T absorption spectrum and various rate constants are known; in the second case, rhodamine B, the T-T spectrum is known but not the rate of intersystem crossing. By comparing

the observed laser threshold and frequency for the latter case with values predicted using various choices of k_{ST} , limits can be set on the range of possible crossover rates. In both cases the T-T spectrum was measured for a solvent different from that used for the lifetime, quantum yield, and fluorescence spectrum. This, combined with large uncertainties in the T-T extinction coefficients, necessarily limit any quantitative predictions. The triplet lifetimes are assumed to be long compared to the fluorescence lifetimes and the duration of the pumping pulse.

a. Anthracene

Anthracene was chosen for analysis since its triplet spectrum has been studied extensively.²⁰ The singlet fluorescence spectrum for anthracene in cyclohexane²¹ and a portion of the triplet absorption spectrum²² which overlaps it are shown in Fig. 15. The fluorescence function $f(\omega)$ was scaled using $\tau_S = 4.9$ nsec and $\phi = 0.36$ in Eq. (6) and $\mu = 26,500$ cm^{-1} .²¹ For excitation, the second harmonic of a ruby laser at 3472\AA and a pulse shape $\gamma(t)$ given in Fig. 19 were considered. The rate of intersystem crossing for anthracene in benzene has been measured²³ and corresponds to $\eta = 0.13$; a value of $\eta = 0.1$ was used in the present calculations. The triplet lifetime, which can be strongly affected by the presence of quenching impurities, was assumed to be greater than 1 μsec and hence relaxation from T_1 to S_0 is negligible on the time scale of the pumping and singlet decay. The rate equations in Eq. (9) were solved under the above conditions.²⁴ The resulting time-varying fractional populations in the singlet and triplet levels are included in Fig. 16. Whereas the singlet population increases and decreases with only a small time lag with respect to γ , the triplet population exhibits a continual increase and approaches $\sim 20\%$ of the total population for a pumping intensity of $\gamma_{\text{max}} = 1.0$.

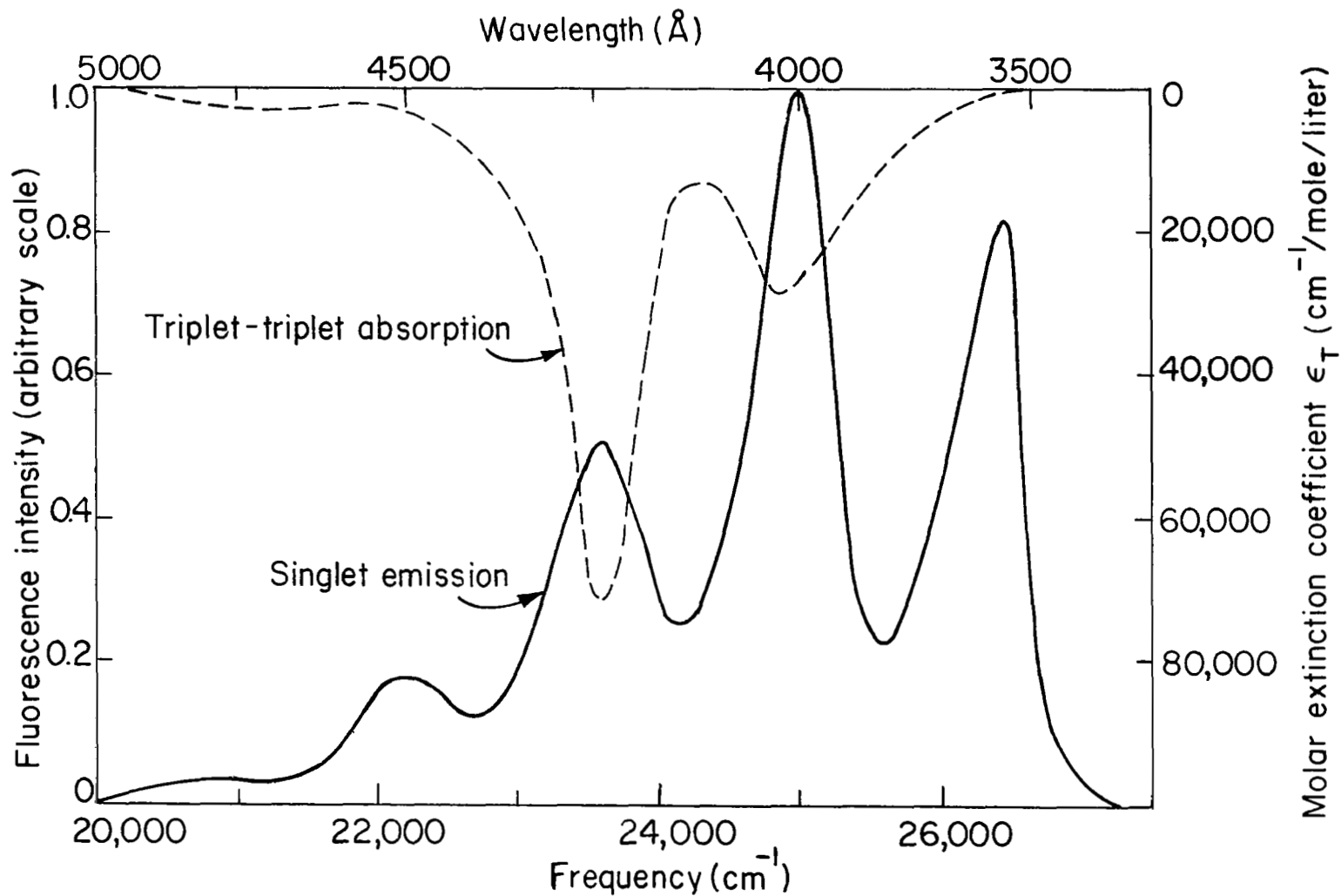


Fig. 15 Singlet Fluorescence Spectrum (Ref. 21) and Triplet-Triplet Absorption Spectrum (Ref. 22) for Anthracene

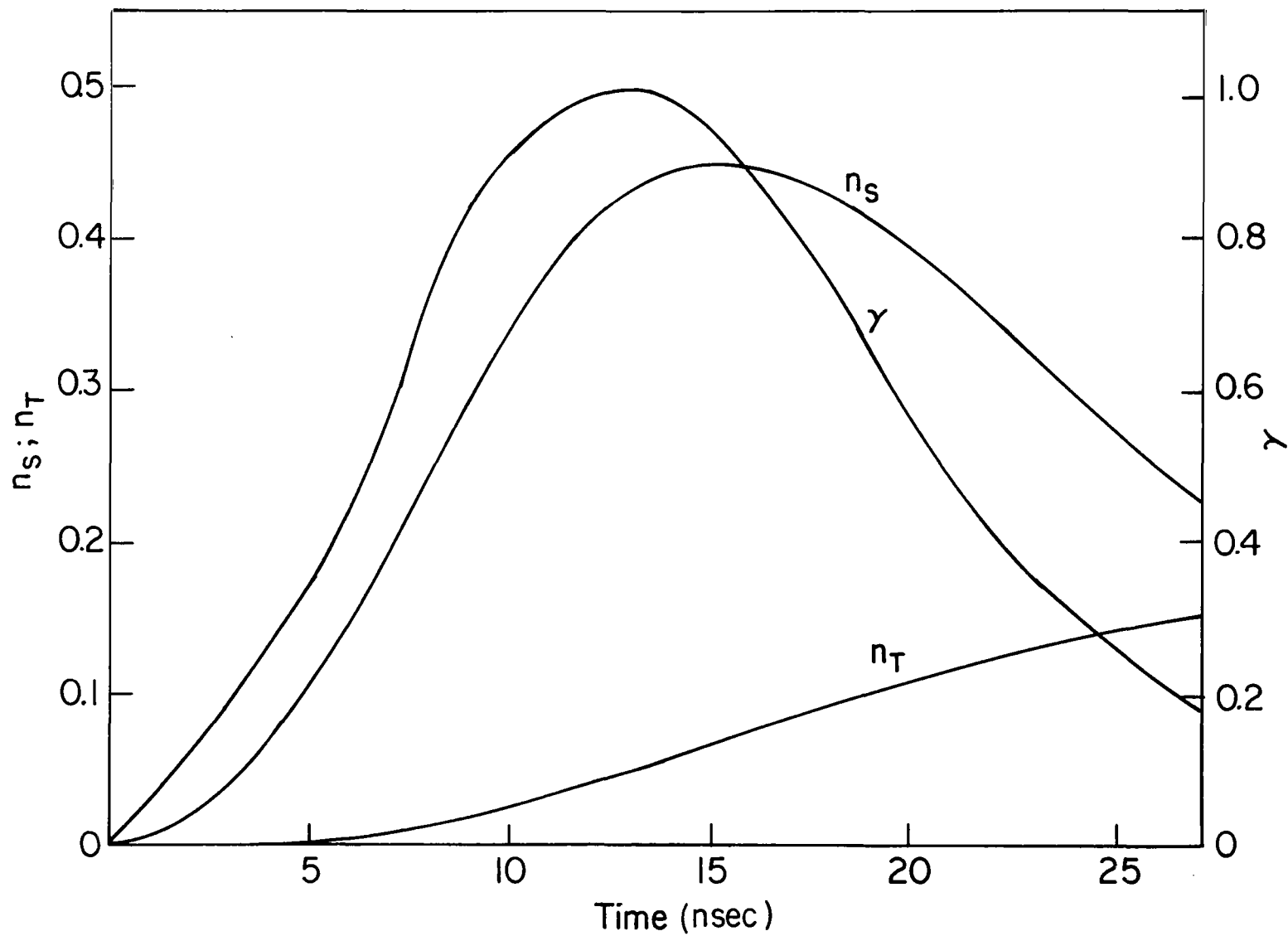


Fig. 16 Calculated Time Variations of the First Excited Singlet and Triplet Level Populations of Anthracene for a Pumping Pulse $\gamma(t)$. In Eq. (9) $\tau_S = 4.9$ nsec, $\eta = 0.1$, and $\rho \approx 10^{-3}$.

The buildup of the triplet population and the strong T-T absorption peak at $23,500\text{ cm}^{-1}$ dramatically affect the gain in this spectral region. This is seen from the gain curves at various times during the pumping pulse shown in Fig. 17. Shortly after pumping begins, the maximum gain is obtained at $23,600\text{ cm}^{-1}$. As pumping proceeds, the gain maximum jumps discontinuously to $25,000\text{ cm}^{-1}$. The gain then continues to increase as n_S increases until the population accumulation in the triplet state and associated absorptive losses become important. The onset of significant T-T losses is first apparent as a small dip in the gain curve at $\approx 23,500\text{ cm}^{-1}$ for $t = 14.4\text{ nsec}$. The continued growth of n_T soon makes the gain negative in this region and, at latter times, in other spectral regions as well.

Sorokin et al.⁹ estimated that to achieve laser action in anthracene at $\approx 25,000\text{ cm}^{-1}$, the pump source should reach its maximum at a time less than $\sim 5 \times 10^{-9}\text{ sec}$; hence excitation via a giant pulse laser would be required.²⁵ Their estimate was based upon the extreme case that all nonradiative decay was intersystem crossing, that is, $\eta = 0.64$, whereas $\eta = 0.1$ was used in above calculations. For the assumption $\eta = 0.64$, the triplet population buildup is much faster and large regions of negative gain appear much sooner. Isolated regions of positive gain, such as at $t = 30\text{ nsec}$ in Fig. 17, do remain, however.

b. Rhodamine B

In an earlier letter,¹⁰ the gain characteristics of rhodamine B in methanol for flashlamp versus laser pumping were compared. Gain calculations were performed neglecting the triplet system, although its possible importance in the flashlamp-pumped case was acknowledged. Buettner²⁶ has recently measured the T-T absorption spectrum of rhodamine B in polymethylmethacrylate. The triplet spectrum,²⁶ together with the absorption and fluorescence spectrum of $5 \times 10^{-5}\text{ M}$ rhodamine B in methanol, are shown in

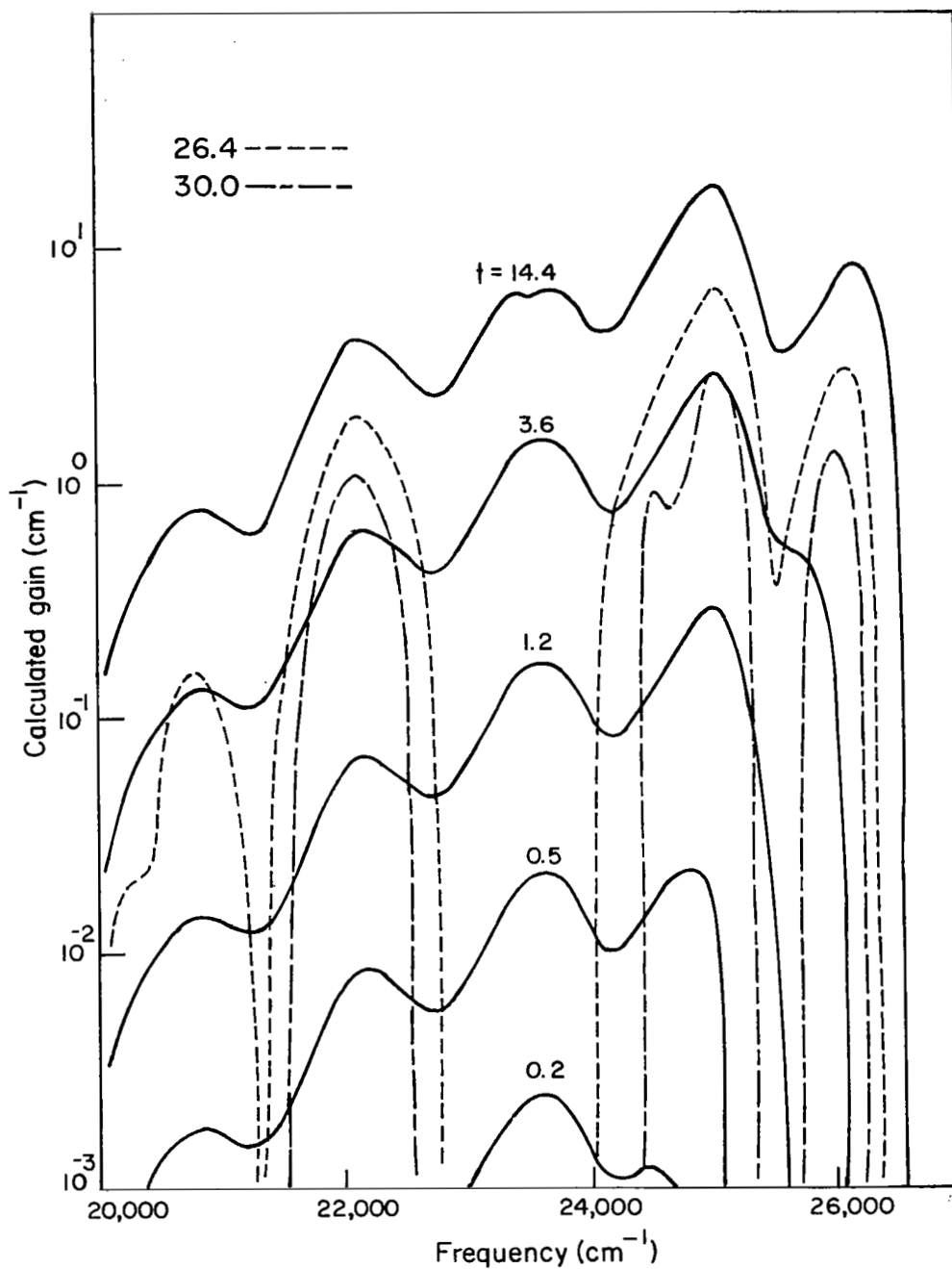


Fig. 17 Calculated Gain as a Function of Frequency for Anthracene at Various Times During the Pumping Pulse Shown in Fig. 16

Fig. 18. Although the T-T spectrum in methanol may be somewhat different, we shall use Buettner's curve as shown. The dashed portion of the curve is an extrapolation used in the gain calculations.

The lifetime and quantum yield for the first excited singlet state of rhodamine B in ethanol are 2.0 nsec and 0.39 respectively;¹⁸ these values are used in the calculations below. The rate of intersystem crossing, however, has not been determined to our knowledge. Calculations were therefore made using several different values of η ranging from 0 to 0.61. The triplet population buildup is very dependent upon the branching ratio for decay from S_1 . In Fig. 19, the flashlamp function γ and resulting singlet and triplet level populations are shown for several different η values. Observe that when η is large, the maximum value of n_S occurs before the peak of γ . Therefore here, and in case II discussed earlier, the maximum gain for long pumping pulses is not necessarily coincident with the peak of the pumping intensity. This is in contrast to the behavior shown in Fig. 8 where there is no population transfer from the singlet system.

Gain curves $G(\omega)$ for $5 \times 10^{-5} M$ rhodamine B in methanol were computed as described previously using the flashlamp curve in Fig. 19 and a peak pumping intensity $\gamma_{\max} = 10^{-2}$. For $\eta \gtrsim 0.4$ the T-T losses predominate to the extent that for practical purposes, the gain is always negative. Gain curves for smaller values of η are shown in Figs. 20, 21, 22. These figures reveal the sensitivity of the shape of the over-all gain curve and region of possible laser action to the rate of intersystem crossing. Since the T-T losses make a larger relative contribution to gain reduction in the low frequency, low gain portion of the fluorescence spectrum, changes due to the triplet population appear initially in this region. Note that in Ref. 10 we were unable to obtain laser action at the lower frequencies although the gain curves calculated neglecting triplet effects suggested that lasing should be possible.

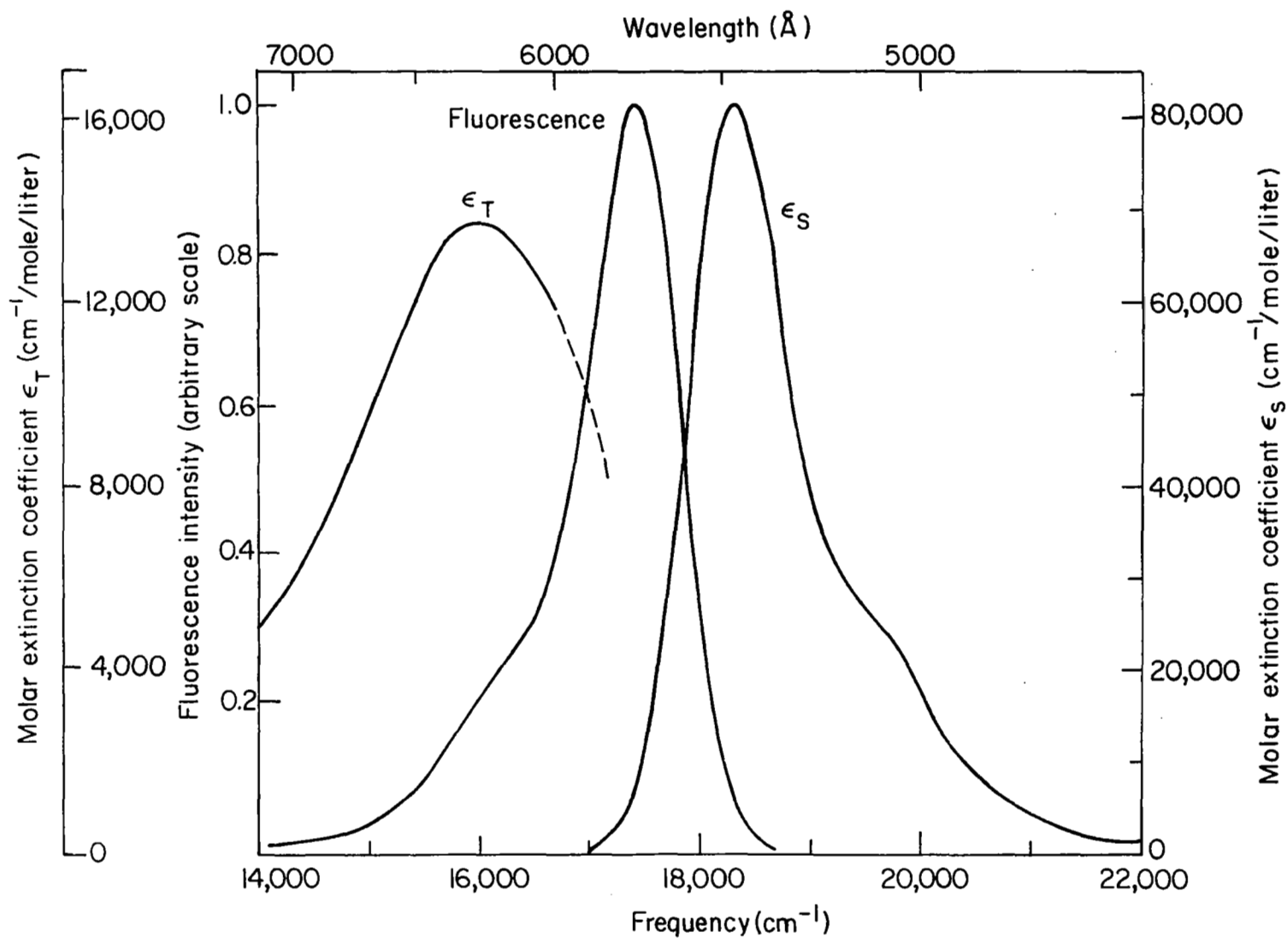


Fig. 18 Singlet Absorption and Fluorescence Spectra of $5 \times 10^{-5} M$ Rhodamine B in Methanol and Triplet-Triplet Absorption Spectrum (Ref. 26) in Polymethylmethacrylate.

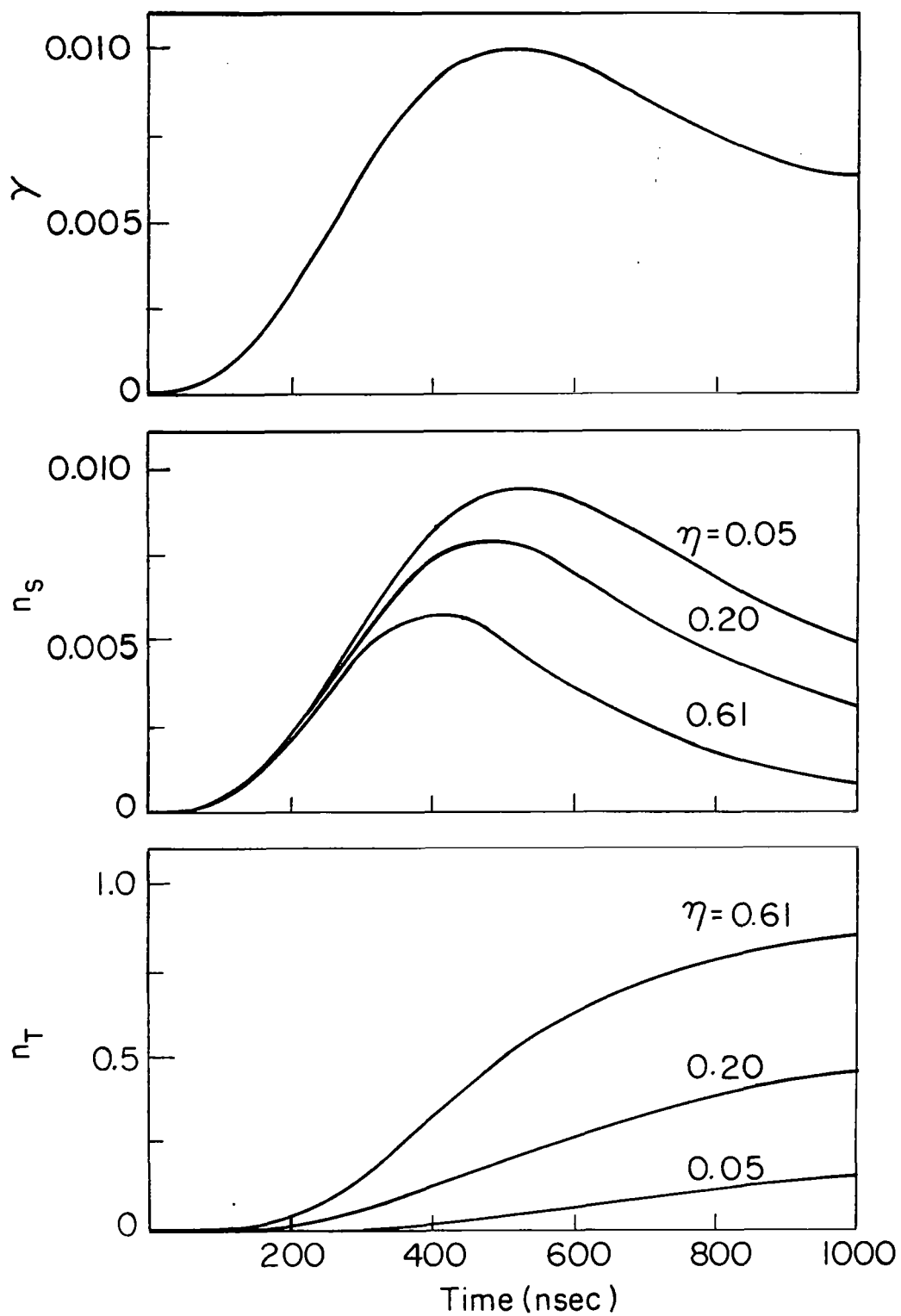


Fig. 19 Flashlamp Pumping Function ($\gamma(t)$) and Calculated Excited Singlet and Triplet Level Populations n_S and n_T of Rhodamine B for Different Choices of Intersystem Crossing Parameter $\eta = k_{ST}\tau_S$. $\tau_S = 2.0$ nsec.

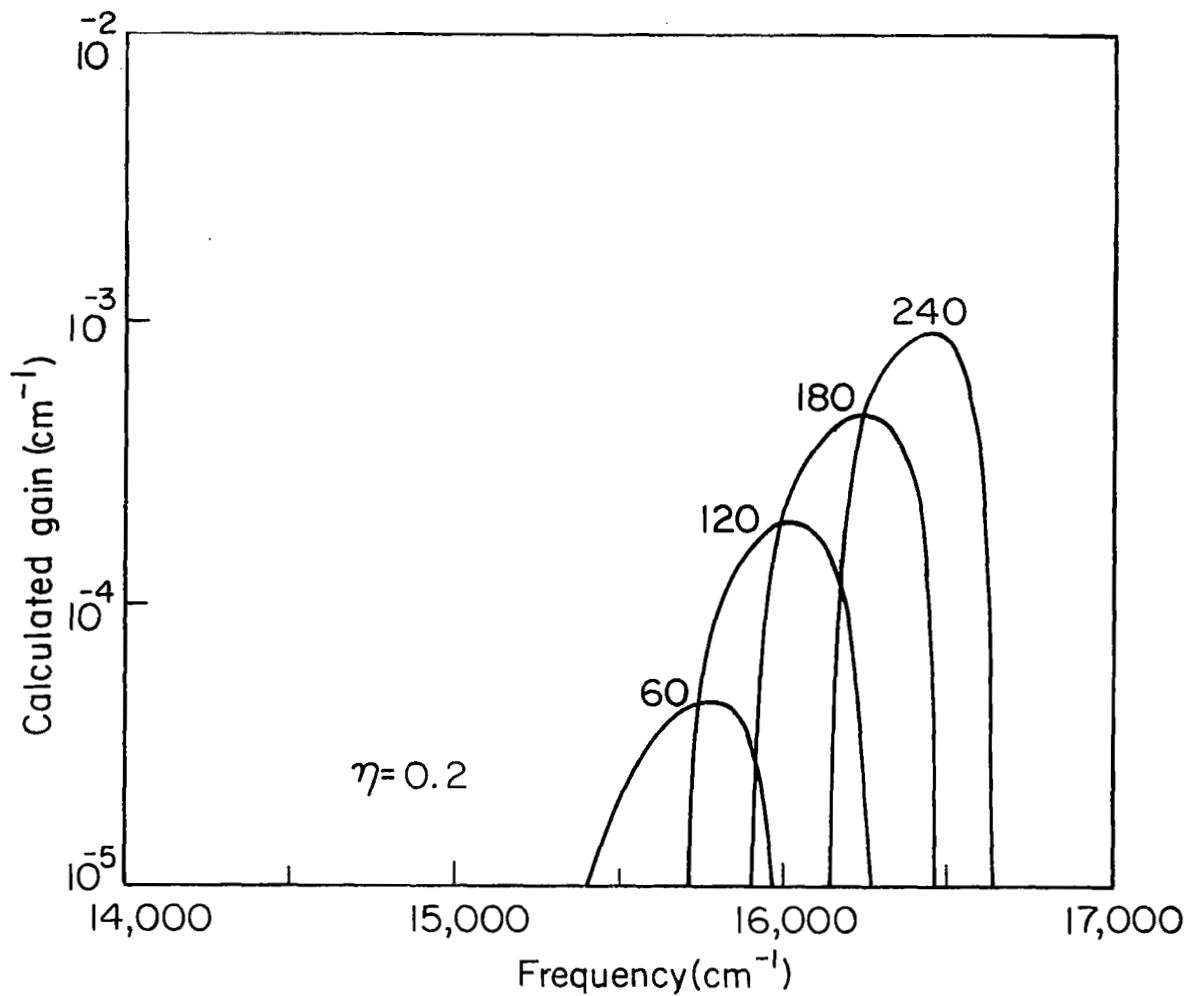


Fig. 20 Calculated Gain Curves for Rhodamine B at Various Times During Flashlamp Pumping (see Fig. 19). Intersystem Crossing Parameter $\eta = 0.2$

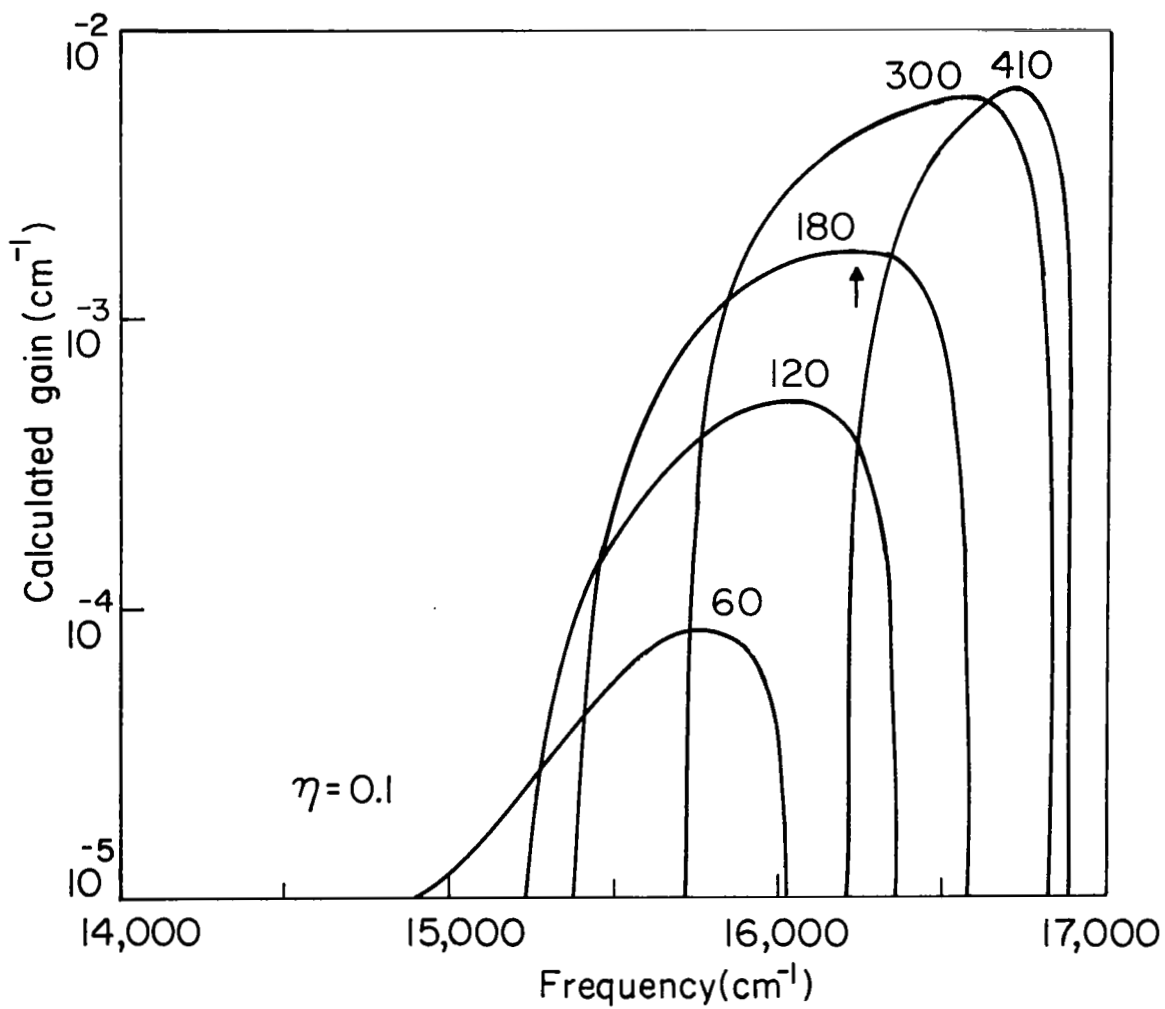


Fig. 21 Calculated Gain Curves for Rhodamine B at Various Times (nsec) During Flashlamp Pumping (see Fig. 22). Intersystem Crossing Parameter $\eta = 0.1$

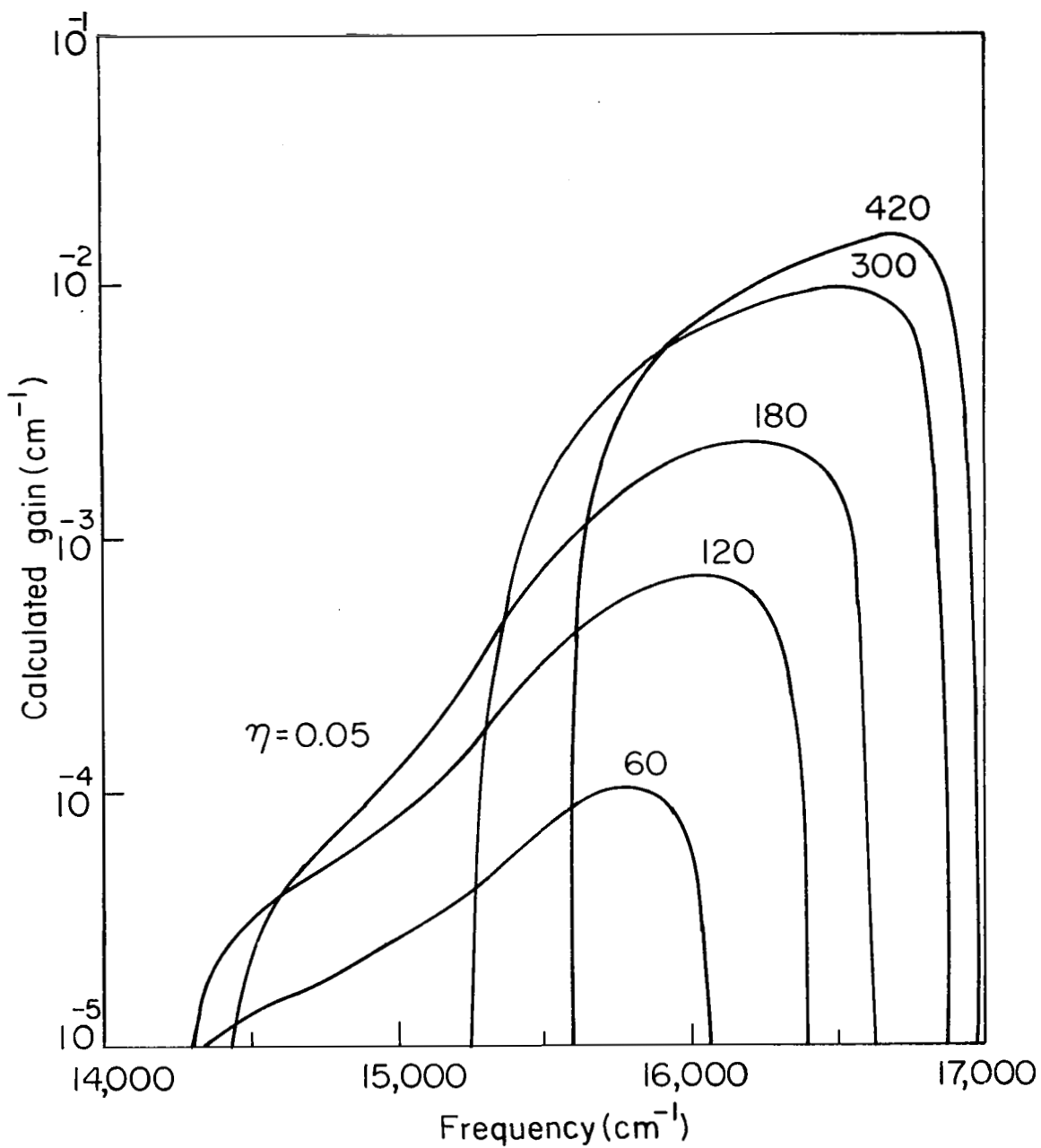


Fig. 22 Calculated Gain Curves for Rhodamine B at Various Times During Flashlamp Pumping (see Fig. 19). Intersystem Crossing Parameter $\eta = 0.05$.

In experiments using a flashlamp-pumped solution of rhodamine B, lasing was recorded at $\approx 16,250 \text{ cm}^{-1}$ approximately 200 nsec after initiation of pumping. The cavity losses were $\sim 3.5 \times 10^{-3} \text{ cm}^{-1}$ and the estimated pumping rate corresponded to $\gamma_{\text{max}} \sim 10^{-2}$. Inspection of Fig. 21 indicates that for $\eta = 0.1$ the peak in the gain curve has the required value for lasing and the frequency and time at which threshold gain is reached are approximately correct (see arrow). For $\tau_S = 2 \text{ nsec}$, this corresponds to a k_{ST} value of $5 \times 10^7 \text{ sec}^{-1}$. Thus measurements of the time and frequency at the threshold for laser action can be combined with calculated gain curves to obtain estimates of the rate of intersystem crossing. The accuracy achievable is dependent, of course, upon how well the T-T absorption intensity²⁷ and other parameters are known.

5. Flashlamp Pumping Criterion

For dyes in which the effects of triplet absorption are important, it is essential that the pumping rate be sufficient to achieve lasing threshold before these losses become dominant. While this is usually not a significant consideration for Q-switched laser pumping, it can be for flashlamp pumping. Criteria for the latter can be derived from the preceding gain expressions. Neglecting absorption from S_1 , Eq. (4) can be rearranged as follows:

$$G(\omega) = N_S [e^{\Omega} + 1] \sigma_0(\omega) - N_T [\sigma_T(\omega) - \sigma_0(\omega)] - N\sigma_0(\omega) \quad (16)$$

Since we shall be interested in cases where $\sigma_T(\omega) > \sigma_0(\omega)$ in the fluorescence region, the second term on the right is negative. Therefore, because of the continual population accumulation in the metastable triplet level during optical pumping, laser action is possible only if threshold gain is reached before the triplet loss term, $N(t)[\sigma_T(\omega) - \sigma_0(\omega)]$, becomes equal to the singlet gain term, $N_S(t) [e^{\Omega} + 1] \sigma_0(\omega)$, in Eq. (16),

Sorokin et al.^{28,9} have discussed the above characteristics of dye lasers previously and have given an expression for the time T_ℓ at which the singlet gain and triplet loss terms become equal. A flashlamp which had an intensity increasing linearly up to a maximum at time T_m was considered. Assuming an effective pumping rate $P_0 t$ for $0 \leq t \leq T_m$ and weak pumping, $N_S(t) \approx NP_0 \tau_S t$ and $N_T(t) \approx NP_0 k_{ST} \tau_S t^2 / 2$. Using these values in Eq. (16), the critical time becomes

$$T_\ell(\omega) = \frac{2(e^{\Omega} + 1) \sigma_0(\omega)}{k_{ST}[\sigma_T(\omega) - \sigma_0(\omega)]} \quad (17)$$

For the special case of mirror-image absorption and fluorescence spectra, where $\sigma_0(\omega) = \sigma_0(2\omega_0 - \omega) e^{-\Omega}$, and in the further limits of $e^{-\Omega} \ll 1$ and $\sigma_T(\omega) \gg \sigma_0(\omega)$, Eq. (17) reduces to

$$T_\ell(\omega) = \frac{2}{k_{ST}} \frac{\sigma_0(2\omega_0 - \omega)}{\sigma_T(\omega)} \quad (18)$$

This is the result presented previously by Sorokin et al.⁹ As an example, $T_\ell(\omega)$ is plotted as a function of frequency in Fig. 23 using the preceding data for rhodamine B. The figure illustrates the large variation of $T_\ell(\omega)$ that may occur throughout the fluorescence region.

Recently, in evaluating potential candidates for flashlamp-pumped organic-dye lasers, the criterion was imposed that for a flashlamp rising linearly in time and attaining its maximum intensity at T_m , laser action is possible only if $T_m < T_\ell$.⁹ This condition is relevant to efficient pumping or for a constant energy flashlamp. In general, however, it is neither a necessary nor a sufficient condition. If the threshold gain for oscillation can be obtained for a flashlamp having $T_m < T_\ell$, then a similar, more energetic lamp having the same or larger pumping rate will likewise achieve lasing even though its peak intensity may occur at a time greater than T_ℓ . At the other extreme, $T_m < T_\ell$ is not a sufficient condition since obviously the pump power must also be adequate to reach threshold gain.

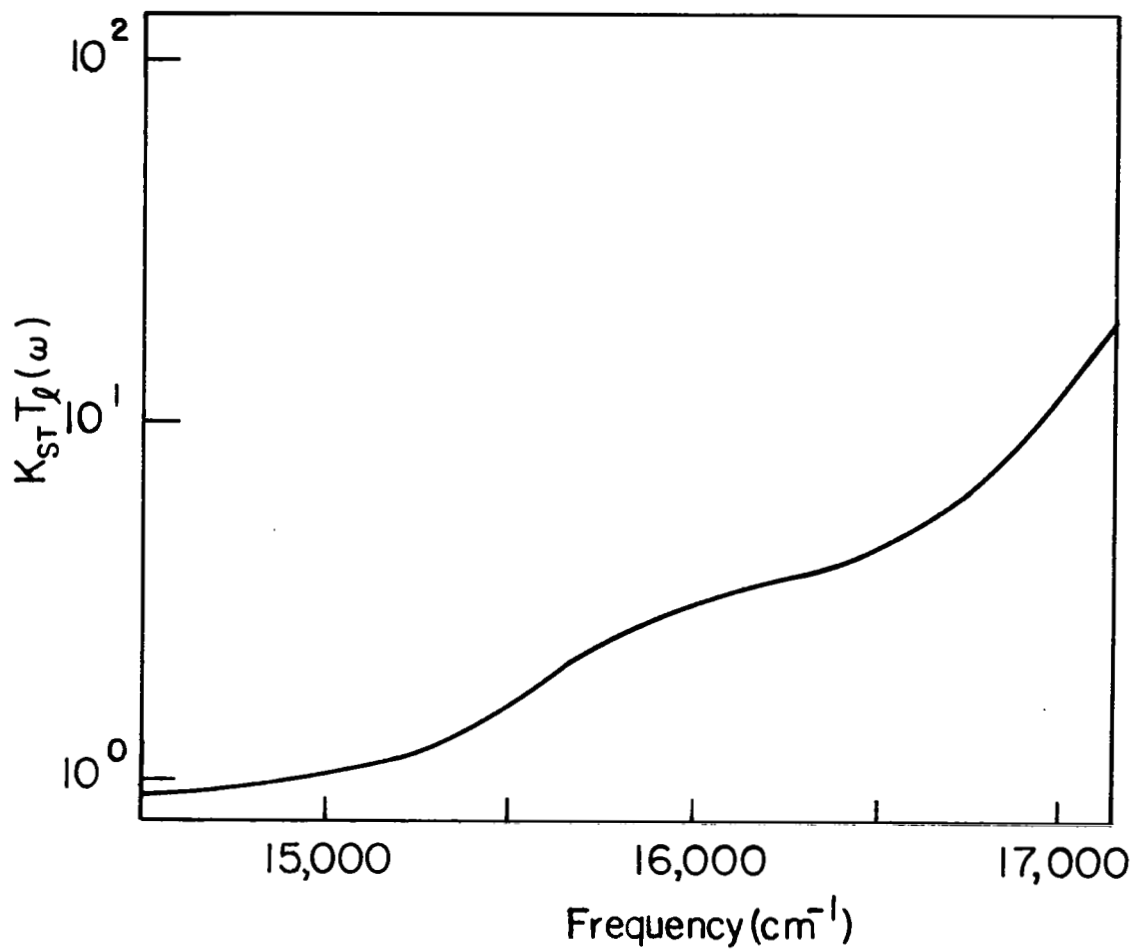


Fig. 23 $k_{ST} T_l(\omega)$ vs ω from Eq. (18) for Rhodamine B.

To achieve laser action, it is the integrated pumping intensity within some characteristic time which is important. We illustrate this by considering a pumping pulse $P(t) = P_0 \sin(\pi t/2T_m)$ for $0 \leq t \leq 2T_m$, again in the limit of weak pumping. For this lamp, the gain in Eq. (16) is maximum at a time

$$t_{\max} = \frac{2T_m}{\pi} \tan^{-1} \left[\frac{\pi T_d}{4T_m} \right], \quad (19)$$

where T_d is a parameter characteristic only of the dye and is defined by

$$T_d(\omega) = \frac{2(e^{\Omega} + 1) \sigma_0(\omega)}{k_{ST} [\sigma_T(\omega) - \sigma_0(\omega)]}. \quad (20)$$

For a constant Q laser cavity, threshold gain must be reached by t_{\max} . Note that here the time of maximum gain depends both upon the dye, via T_d , and upon the lamp pulse, via T_m . In contrast, for a flashlamp having a linearly increasing pumping flux, $t_{\max} = T_d/2$ (or $T_d/2$ since $T_d = T_d$).²⁹ The minimum pumping rate required to achieve laser action is found by setting the gain at t_{\max} equal to the threshold gain G_{thres} and is given by

$$P_0 = \frac{\pi}{2T_m} \frac{G_{\text{thres}}(\omega) + N\sigma_0(\omega)}{Nk_{ST}\tau_S [\sigma_T(\omega) - \sigma_0(\omega)]} \left\{ \left[1 + \left(\frac{\pi T_d}{4T_m} \right)^2 \right]^{\frac{1}{2}} - 1 \right\}^{-\frac{1}{2}}. \quad (21)$$

Using this result, the minimum number of pumping photons that must be absorbed in a time t_{\max} after initiation of pumping is

$$N \int_0^{t_{\max}} P(t) \cdot dt = \frac{\left[G_{\text{thres}}(\omega) + N\sigma_0(\omega) \right] \left[1 + \left(\frac{\pi T_d}{4T_m} \right)^2 \right]^{-\frac{1}{2}}}{k_{ST} \tau_S [\sigma_T(\omega) - \sigma_0(\omega)]}. \quad (22)$$

Numerical estimates of the corresponding pump powers required to achieve lasing for a typical dye are in agreement with results given earlier.²⁸ The conditions imposed by Eqs. (19-22), while rigorously applicable only to sine-shaped pulses, clearly demonstrate that the criteria for successful flashlamp pumping involve an interdependence on properties of both the lamp and the dye.

Since for broadband dye fluorescence and laser cavities the frequency at which the gain is a maximum may vary with time, estimates of lasing conditions made using the above types of expressions are uncertain because one does not know a priori what frequency (ω) to use. The above treatment and Eqs. (19-22) were presented to expose explicitly some of the problems involved in selecting flashlamp parameters. Whenever the flashlamp pulse shape, cavity losses, and spectroscopic properties of the dye of interest are known, it is preferable to calculate $G(\omega)$ curves for various pumping rates $P(t)|_{\max}$ until the peak gain obtained is sufficient to achieve oscillation. In this manner the time and frequency at threshold and the minimum energy required for lasing can be found simultaneously.

6. Concluding Remarks

The gain characteristics of dye lasers have been calculated by treating them as four-level laser systems; rapid equilibration among the vibrational levels was assumed and population transfer to the triplet level system and associated losses were included. The treatment reveals the time evolution of the gain, the dependence of the laser frequency on cavity Q , and, from experiments using rhodamine 6G, how the lasing frequency may be tuned by the introduction of an intracavity Q switch. When intersystem crossing is negligible, a master set of gain-vs-frequency curves can be constructed for various excited-state population values. These, combined with solutions of the population rate equations for a given pump pulse, can be used to predict the frequency and time at threshold for a laser cavity of known losses. When triplet losses are important, however, no single set of gain curves suffices for all pump pulses but must be calculated for each individual case.

Knowledge of several spectroscopic properties is prerequisite to the successful application of the theory to a particular dye. These properties include absorption and fluorescence spectra, lifetimes of

the excited singlet and triplet states and fluorescence quantum efficiency. These quantities must also be appropriate to the host, dye concentration, and temperature of interest. Because radiation trapping effects may be present in an actual laser configuration, the effective trapped lifetime is required in the population rate equations; in evaluating the fluorescence function $f(\omega)$, however, the true radiative lifetime is required.

Application of the theory to predict the threshold conditions for a given laser configuration requires, in addition, knowledge of cavity losses and the time and intensity characteristics of the pump source. In practice, these properties usually cannot be determined precisely because of geometric factors affecting the net absorption and scattering. The accuracy of the threshold predictions are accordingly limited.

Comparison of computer-calculated vs observed laser threshold conditions can be used to obtain estimates of the rates of intersystem crossing, as was shown in the case of rhodamine B, and to establish the importance and the spectral distribution of triplet loss mechanisms. In cases of overlapping fluorescence and triplet absorption spectra, such as anthracene, it would be of interest to examine those spectral regions where lasing could be obtained at later times even when n_T is large. A Q-switch in the laser cavity, as used in the experimental arrangement in Fig. 14, could be opened at various times after pumping began and the lasing spectrum probed by using a grating or other intracavity frequency-selecting element.

B. Additional Experiments

The scheme for pumping dyes with linear lamps as demonstrated by Schäfer⁴ and sketched in Fig. 3 involves operation of the lamp at voltages above that at which it breaks down. The spark gap prevents lamp breakdown and permits storage of the appropriate energy on the low capacitance, high-voltage capacitor. This arrangement of circuit elements gives pulses with fairly short risetimes ($\sim 1 \mu\text{sec}$).

We decided to try a variation of Schäfer's scheme by using a higher capacitance at lower voltage to store the pump energy. The operating voltage was below the lamp breakdown voltage and so parallel triggering could be employed and no energy wasted in the spark gap. We used a PEK Labs XE1-3 lamp, a Maxwell Labs $5.5 \mu\text{f}$, 5kV , $\sim 10 \text{nh}$ capacitor and a 3 in. silver-plated elliptical cavity with the dye at one focus and the lamp at the other. This system produced a light pulse which peaked in $\sim 2 \mu\text{sec}$ and was able to excite lasing in ethanol solutions of rhodamine 6G, rhodamine B, acridine red, and pyronin B. The threshold for a 10^{-4}M rhodamine 6G solution was $\approx 14 \text{J}$ using broadband 100 and 99 percent R cavity mirrors. We feel that this will be substantially lowered when a dye cell with more carefully aligned windows is obtained. When the lamp was water cooled and the dye flowing through the cell, we were able to operate this system at repetition rates up to 20 pps before the need for cooling the dye supply arose.

A number of attempts were made to find new dye laser materials, with particular emphasis on the blue region of the spectrum. The dyes were tried in annular flashlamps with one or more of several different capacitors, namely a $2.2 \mu\text{fd}$ - 12kV , a $0.18 \mu\text{fd}$ - 50kV , and a $0.3 \mu\text{fd}$ - 25kV unit. The optics consisted of 100 and 99 percent R mirrors at the wavelengths of interest. The dyes tried unsuccessfully are listed in Table II. Table I lists results on several in which laser action was previously observed elsewhere, and two which have only recently been reported -- 7 diethylamino-4 methylcoumarin²⁸ and pyronin B.²⁹

TABLE II. Compilation of dye-solvent combinations which did not laser in the annular flashlamp. Mirror reflectivities of 100% and 99.5% were used.

Dye	Solvent	Conc.	Energy in joules
1-aminonaphthalene	ethanol	10^{-4}	90
"	cyclohexane	10^{-4}	90
9-amino acridine hydrochloride	ethanol	10^{-4}	90
" " "	H ₂ O	$10^3, 10^{-4}$	110
4-phenyl -7-hydroxy coumarin	ethanol	10^{-4}	90
3-phenyl coumarin	ethanol	10^{-4}	90
4-OH-3-COOEth coumarin	ethanol	10^{-4}	90
p-terphenyl	cyclohexane	10^{-4}	90
perylene	cyclohexane	10^{-4}	90
Pyronin Y	ethanol	10^{-4}	90
"	"	$.5 \times 10^{-4}$	
Rubrene	benzene	10^{-3}	110
9, 10 diphenyl anthracene	benzene	10^{-4}	110
	ligroin	10^{-3}	110
triphenylethylene	methanol	$10^{-3}, 10^{-4}$	110

IV. CONCLUSIONS

The main conclusions reached during this work are given in Sec. III. A where they are presented in the context of our theoretical and experimental work. We have developed a method of analysis for dye lasers which permits us to explain most of their properties. As part of this work we have shown that the effectiveness of a particular dye-flashlamp combination depends in a complicated manner on both dye and flashlamp properties. This interdependence makes it inappropriate to select flashlamp parameters by assuming a simple pump-pulse shape and estimating therefrom the input energy requirements. Indeed, it is more useful in cases where the required dye and flashlamp properties are known to compute the time- and frequency-dependent gain for various pumping rates in order to determine the minimum required pump energy. However, there is one general conclusion about flashlamps which provides a useful rule of thumb when designing a dye laser system. It is that for a fixed energy, the pump lamp will be more efficient if the pump pulse is short (i. e. , $< 1 \mu\text{sec}$).

In summary we find that most dye laser properties can be understood through the analysis presented in this report. This approach gives some aid in selecting potential laser candidates and in planning the appropriate pumping procedure. With this analysis available as a tool, future studies of dye lasers should be more easily planned and the results more readily understood.

REFERENCES

1. D. E. McCumber, Phys. Rev. 134, A299 (1964).
2. P. P. Sorokin and J. R. Lankard, IBM J. Res. Develop. 10, 162 (March 1966).
3. P. P. Sorokin and J. R. Lankard IBM J. Res. Develop. 11, 148 (March 1967).
4. F. P. Schäfer, Int'l Quantum Electron. Conf. Paper 4D-5.
5. M. Bass and J. I. Steinfeld, IEEE J. Quantum Electron. QE-4, 53 (Feb. 1968).
6. F. P. Schäfer, W. Schmidt, and J. Volze, Appl. Phys. Lett. 9 306 (Oct. 1966).
7. M. Bass, T. F. Deutsch, and M. J. Weber, to be published Appl. Phys. Lett., August 1968.
8. B. H. Soffner and B. B. McFarland, Appl. Phys. Lett. 10, 266 (June 1967).
9. P. P. Sorokin, J. R. Lankard, V. L. Moruzzi, and E. C. Hammond, "Flashlamp Pumped Organic Dye Lasers," J. Chem. Phys. 48, 4726 (May 1968), a good review of flashlamp-pumped dye lasers and references to previous dye laser studies.
10. M. Bass, T. F. Deutsch, and M. J. Weber, "Frequency- and Time-Dependent Gain Characteristics of Laser- and Flashlamp-Pumped Dye Solution Lasers," to be published in Appl. Phys. Lett., August 1968; included as Appendix B to this report.
11. G. T. Schappert, K. W. Billman, and D. C. Burnham, "Temperature Tuning of an Organic Dye Laser," to be published Appl. Phys. Lett., August 1968.
12. See, for example, J. G. Calvert and J. N. Pitts, Photochemistry (John Wiley and Sons, New York, 1966).
13. Internal conversion and intersystem crossing denote nonradiative transitions between electronic states of the same multiplicity (S-S and T-T) or different multiplicity (S-T), respectively.
14. P. M. Rentzepis, "Direct Measurements of Radiationless Transitions in Liquids, Chem. Phys. Lett. 2, 117 (June 1968), has used intense picosecond light pulses from a mode-locked laser to create a non-equilibrium situation and thereby study nonradiative vibrational relaxation in liquids.
15. B. F. Soffer and B. B. McFarland, "Frequency Locking and Dye Spectral Hole Burning in Q-Spoiled Lasers," Appl. Phys. Lett. 9, 196 (April 1966).
16. C. R. Guillianio and L. D. Hess, "Investigation of Spectral Bleaching in Passive Q-Switch Dyes," Appl. Phys. Lett. 9, 196 (Sept. 1966).

REFERENCES (Cont'd)

17. M. Hercher, W. Chu, and D. L. Stockman, "An Experimental Study of Saturable Absorbers for Ruby Lasers," to be published in IEEE J. Quantum Electronics.
18. B. B. Snavely and O. G. Peterson, "Experimental Measurement of the Critical Population Inversion for the Dye Solution Laser," to be published in IEEE J. Quantum Electronics.
19. P. I. Petrovich and N. A. Borisevich, "Fluorescence Spectra and Efficiencies of Some Coumarin Derivatives," IZV. Akad. Nauk SSSR, Ser. Fiz. 27 (5), 703 (May 1963). The authors report a quantum yield of 0.97 for 7-hydroxycoumarin in water.
20. The Triplet State, ed. A. B. Zahlen (Cambridge University Press, Cambridge, 1967).
21. I. B. Berlman, Handbook of Fluorescence Spectra of Aromatic Molecules (Academic Press, New York, 1965).
22. G. Porter and M. W. Windsor, "The Triplet State in Fluid Media," Proc. Roy. Soc. (London), A245, 238 (December 1957).
23. M. W. Windsor et al., "Research on Triplet States and Photochromism for Flash-Blindness Protection," TRW Systems Annual Report, Contract AF-41 (609)-2425 (April 1965).
24. R. E. Kellogg, "Second Triplet State of Anthracene," J. Chem. Phys. 44, 411 (January 1966). The second triplet level T_2 of anthracene is located very near S_1 , being $\sim 1200 \text{ cm}^{-1}$ below S_1 in solutions but above S_1 in solids. Since transfer $S_1 \rightarrow T_1$, the rate equations in Eq. (11) are still appropriate.
25. Recently, B. G. Huth and G. I. Farmer, "Laser Action in 9, 10 Diphenylanthracene," IEEE J. Quantum Electron. QE-4, 427 (April 1968), obtained laser action in an anthracene derivative, 9, 10 diphenylanthracene, by pumping with approximately 1 MW of second-harmonic power of a Q-switched ruby laser. The quantum yield for this derivative is greater than for anthracene, $\phi \sim 0.8$
26. B. B. Snavely and A. V. Buettner (private communication) have measured triplet-triplet absorption for rhodamine B in methanol and find the peak at 6225 Å. Although a population buildup in the lowest triplet level would be unimportant for the laser-pumped case, a significant accumulation may occur during flashlamp pumping, thus leading to an additional loss at 6225 Å and pursuant modification of the gain curve in Fig. B-1, b.
27. For rhodamine B, the maximum T-T extinction coefficient of 1.4×10^4 was uncertain by $\pm 0.5 \times 10^4$ and was measured using a different solvent.
28. P. P. Sorokin, J. R. Lankard, E. C. Hammond, and V. L. Moruzzi, "Laser-Pumped Stimulated Emission from Organic Dyes: Experimental Studies and Analytical Comparison," IBM J. Res. Develop. 11, 130 (March 1967).
29. This result can also be obtained from Eq. (20) in the limit $T_d \ll T_m$ where the sine pulse is linear.

DYE LASERS: THE THREEPENNY LASER*

M. Bass**
Raytheon Research Division
Waltham, Massachusetts

The active medium in dye lasers is a solution of an organic dye in either a liquid or a plastic host. The first dye laser was demonstrated by Sorokin and Lankard¹ in March 1966; they used a Q-switched ruby laser to excite a solution of chloroaluminum phthalocyanine in ethanol. Dye lasers studied since have been both laser and flashlamp pumped and have emitted at wavelengths from ~ 0.45 to $\sim 1.06\mu\text{m}$. This paper examines the properties of fluorescing dye solutions as they relate to lasing, describes methods used to excite dye lasers, and discusses some of their lasing properties.

The general characteristics of the absorption and emission spectra of dye solutions are shown in Fig. 1. These curves and their relationship to dye laser action can be qualitatively understood by examination of Fig. 2, which shows schematically the energy levels of a dye molecule in solution. Each level represents a particular electronic, vibrational, and rotational state of the molecule. Since the electronic contribution to the energy is by far the largest, these levels are grouped together according to their electronic state and by their net electronic spin, either 0 or 1, into groups of singlets or triplets, respectively. Since it is impossible to represent the exact molecular configuration we shall arbitrarily define the distance from the solid vertical line (on the left in Fig. 2.) to represent the molecular configuration corresponding to that group of levels. Electronic excitation takes place much faster than the molecule's configuration can change, and so absorption and emission are shown vertically in Fig. 2. After absorption from S_0 to S_1 , the molecule relaxes nonradiatively to the lower levels of S_1 whence it can emit a photon of less energy than the one absorbed. This accounts for the Stokes shift of fluorescence from absorption in dye solutions.

*The research reported in this paper was sponsored in part by the Electronics Research Center under NASA Contract NAS 12-635.

**Paper appears in Nerem Record 10, 36 (1968).

Examining Figs. 1 and 2, we see that the dye solution can emit where there is no absorption. The energy level scheme for S-S fluorescence is like that of a four-level laser and suggests the possibility of achieving laser action in these solutions.

The achievement of lasing is hindered by two facts: the radiative lifetimes of most dye solutions are short (in general ~ 5 ns), and intersystem crossing to T_0 is a nonradiative loss mechanism. In addition, T-T absorption may be in the same wavelength range as S-S fluorescence. This may cause a potential dye laser to not lase at all or to self-terminate due to the growth of T-T absorption. To achieve dye lasing it is, therefore, necessary to excite a sufficient population into S_1 before either the T-T absorption becomes large or the excited population decays away. For this reason a pump source must be energetic and fast: thus the first dye laser pumps were other laser beams (Fig. 3). Since laser-pumped lasers are not very practical, flashlamps which could produce flashes of light with energies of ~ 10 to ~ 100 j, with risetimes (time to the peak of the pulse) of ~ 500 ns, were developed. Sorokin et al.² used an annular lamp, shown schematically in Fig. 3b, and a disc-shaped capacitor to achieve the desired flashlamp pulse. We have recently found that, with such a lamp, any capacitor with a high ringing frequency will do. In addition Schäfer et al.³ have obtained laser action by exciting certain dye solutions with a commercial linear flashlamp, as shown in Fig. 3c. We have lased rhodamine 6G in ethanol, as well as the two commercially available plastics listed in Table I, with linear lamp pumping.

In addition to those listed in Table I, there are dye lasers available to fill in almost the entire spectral range from 0.45 to 1.06 μm . The lasing wavelengths of most dye lasers can be tuned over very wide ranges (upwards of 200 \AA) by varying the dye solvent,¹ varying the dye concentration,^{1,4} adjusting the cavity Q,⁵ and by Q-switching the dye laser.⁶

The dependence of the lasing wavelength on cavity Q and Q-switching are dynamic effects arising from the frequency- and time-

dependent gain of the laser. In most dyes the gain, and the wavelength at which it is maximum, changes with the time elapsed since excitation. Figure 4 shows this effect for rhodamine B in methanol. For a given cavity Q a certain gain is required for lasing and so the laser wavelength will be the one which achieves this gain first. Change the cavity Q and there will be a new laser wavelength. Fig. 4 also shows that a Q-switch in the cavity with a variable delay could be used to select the lasing wavelength. In addition, Soffer and McFarland⁷ have demonstrated that, by using a diffraction grating as one of the cavity mirrors, one can narrow the lasing spectrum and select the laser wavelength without sacrificing much of the output energy.

Dye lasers can be used as broadband optical frequency amplifiers.⁸ Figure 5, which shows the amplification of the second Stokes line of toluene by different solutions of DTTC, suggests that dye solution amplifiers may also be useful for certain spectroscopy applications.

Acknowledgments:

The author wishes to acknowledge the very useful contributions of his collaborators, Drs. T.F. Deutsch and M.J. Weber.

References:

1. P. P. Sorokin and J. R. Lankard, IBM J. Res. Develop. 10, 162 (March 1966).
2. P. P. Sorokin and J. R. Lankard, IBM J. Res. Develop. 11, 148 (March 1967).
3. F. P. Schäfer, Int'l. Quantum Electron Conf. Paper 4D-5.
4. M. Bass and J. I. Steinfeld, IEEE J. Quantum Electron QE-4, 53 (Feb. 1968).
5. F. P. Schäfer, W. Schmidt, and J. Volze, Appl. Phys. Let. 9, 306 (Oct. 1966).
6. M. Bass, T. F. Deutsch, and M. J. Weber, to be published Appl. Phys. Let. (August 15, 1968).
7. B. H. Soffer and B. B. McFarland, Appl. Phys. Let. 10, 266 (June 1967).
8. M. Bass and T. F. Deutsch, Appl. Phys. Let. 11, 89 (Aug. 1967).

Figure Captions:

- Fig. 1 Absorption and Emission Spectra of a Dye Solution.
- Fig. 2 Schematic Energy-Level Diagram of a Dye Molecule Showing the Transitions Relevant to Dye Laser Action.
- Fig. 3 Methods of Dye Laser Excitation.
- Fig. 4 Calculated Frequency-Dependent Gain of 5×10^{-5} Rhodamine B in Methanol at Various Times After Pumping Begins. The time dependence and estimated intensity of the flashlamp pump is shown in the insert (from Ref. 6).
- Fig. 5 Spectrographic Evidence of the Amplification of the Second Stokes Shifted Line from Toluene by a Ruby Laser Pumped 10^{-5} M Solution of DTTC in (a) DMSO and (b) Ethyl Alcohol (from Ref. 8).

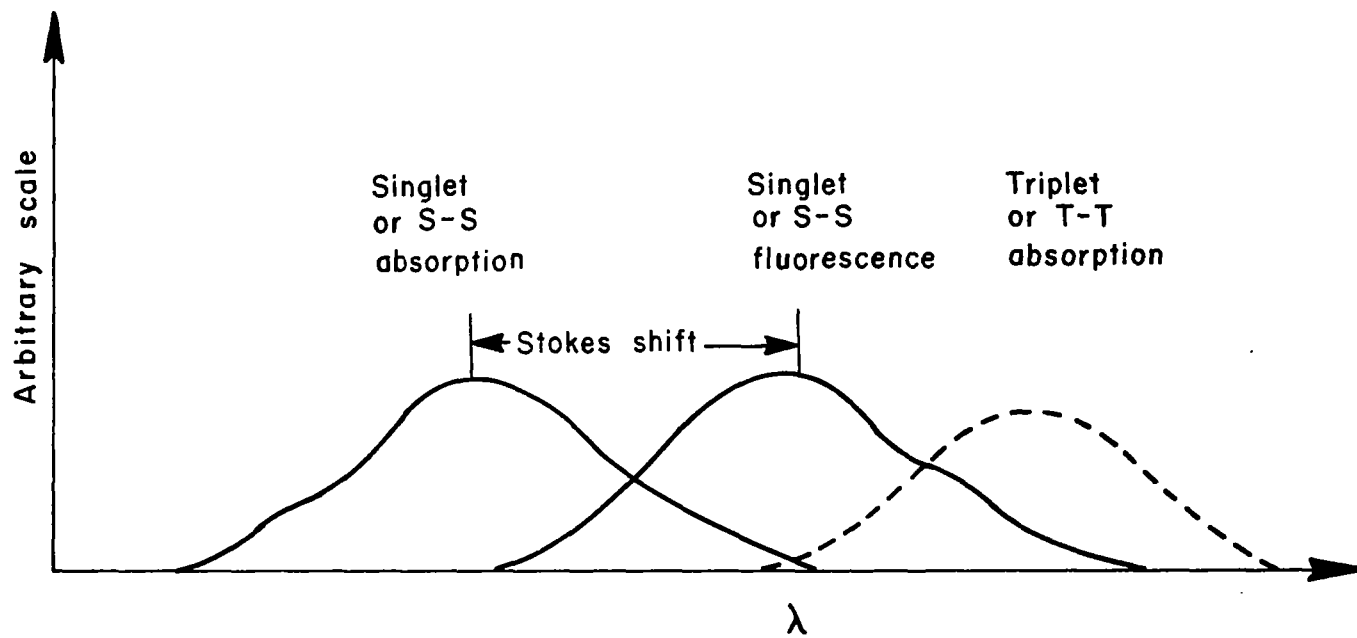


FIGURE 1

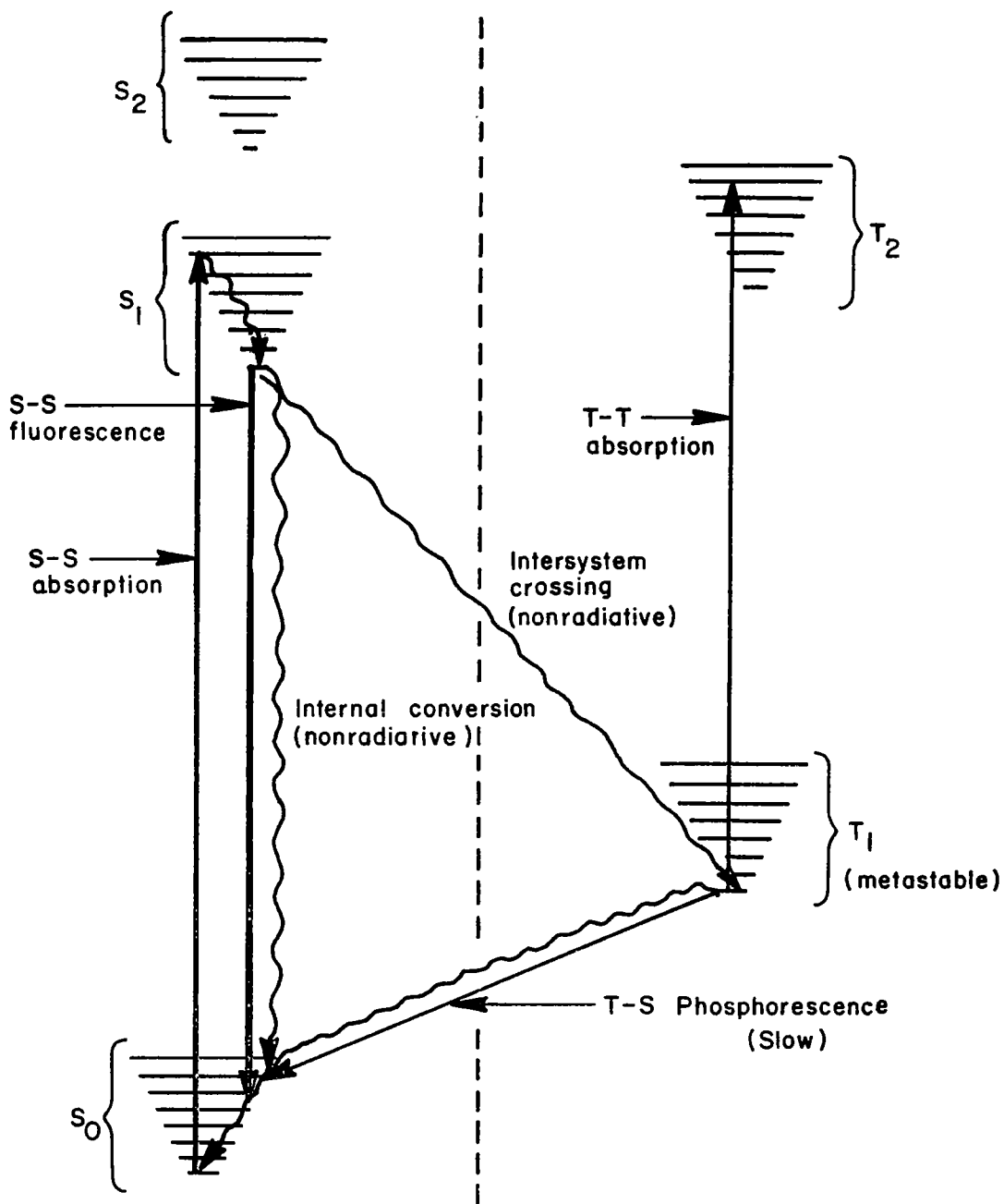


FIGURE 2

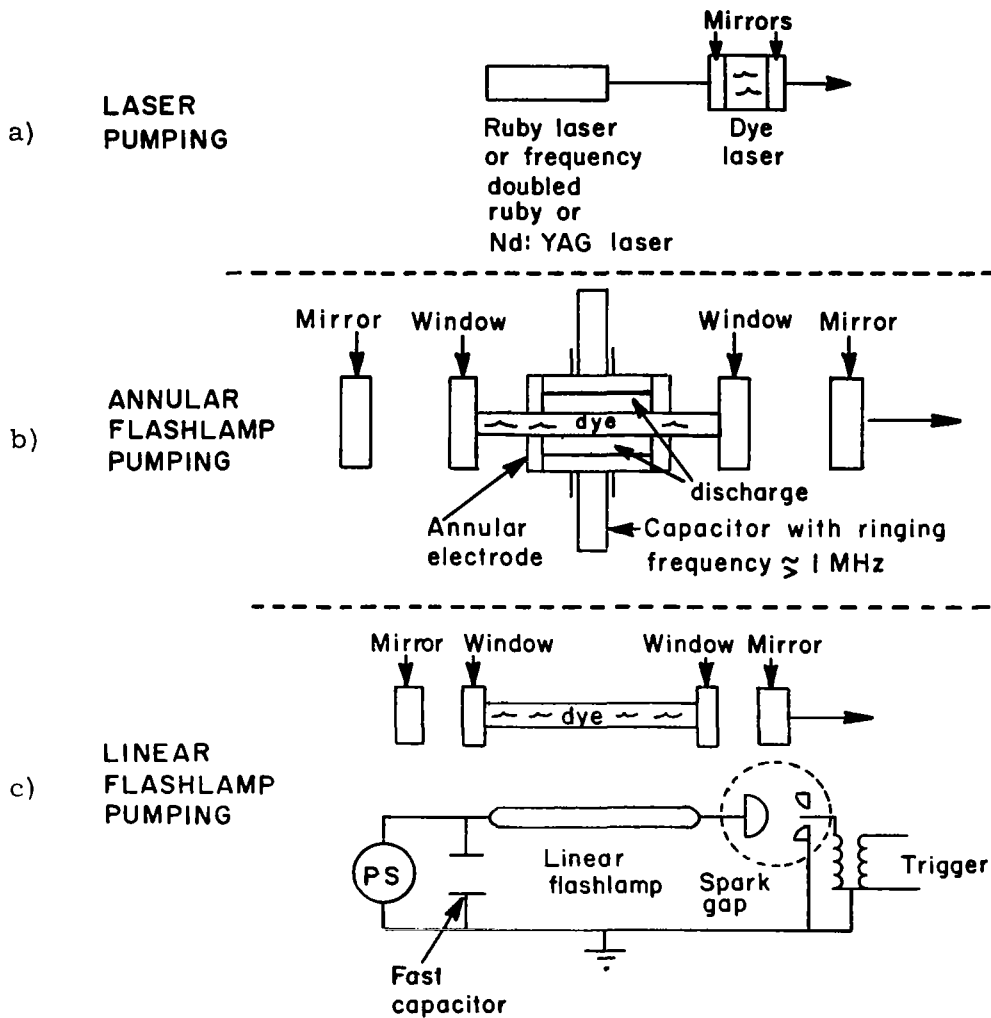


FIGURE 3

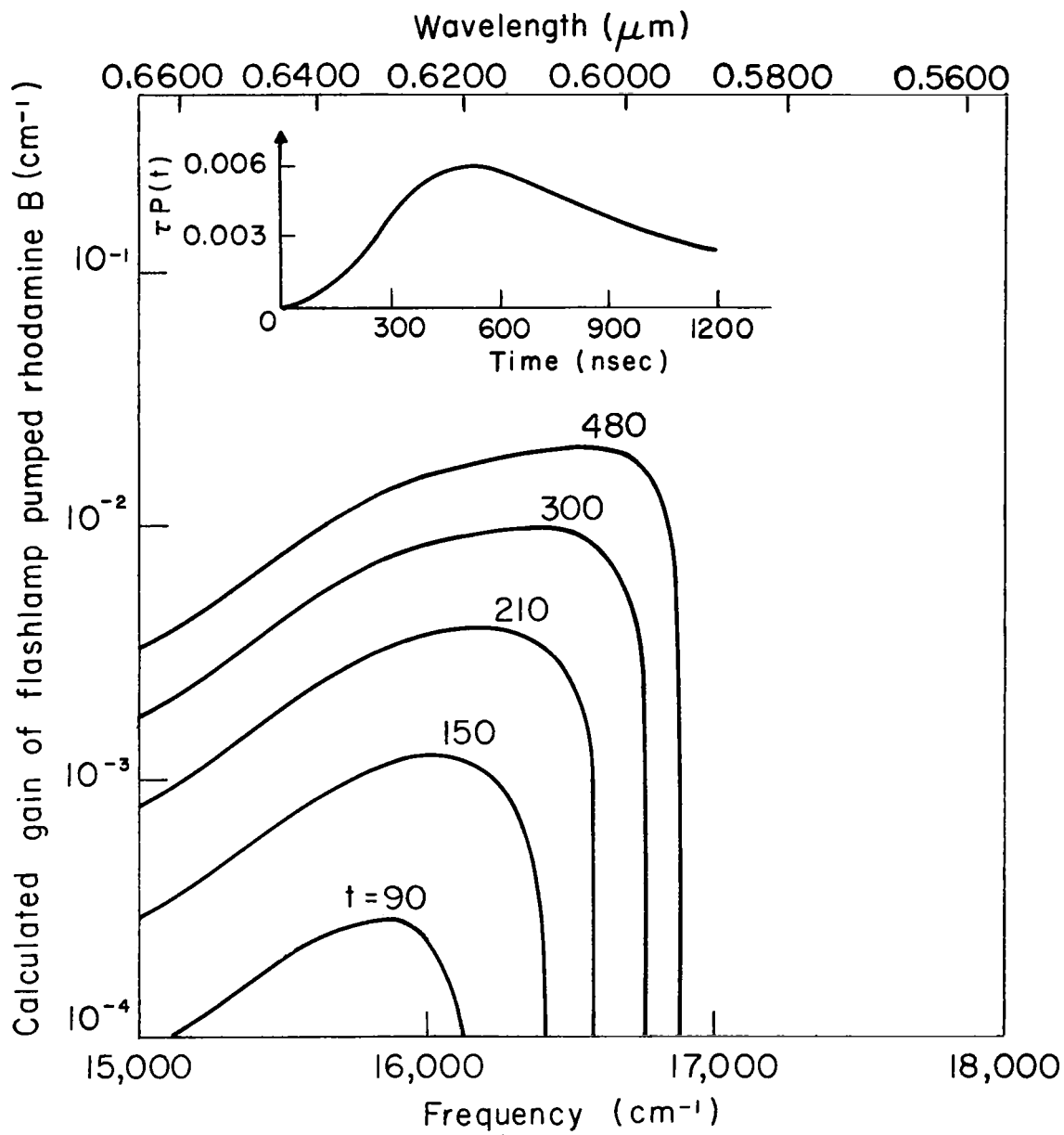


FIGURE 4

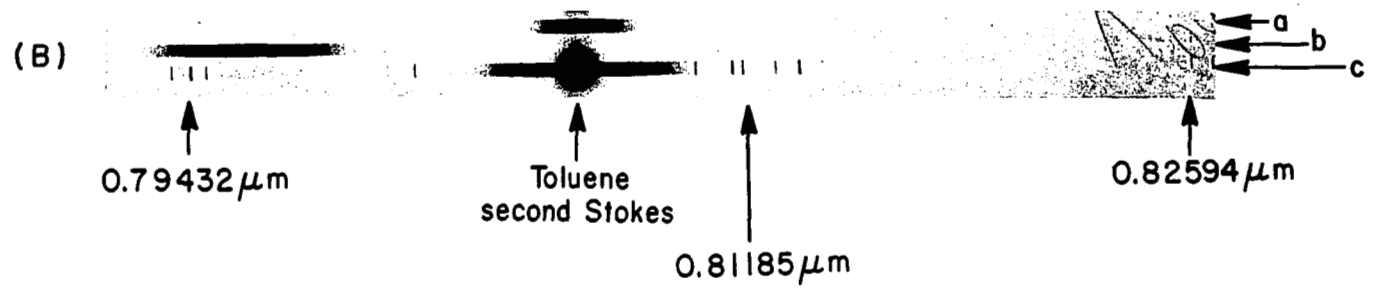
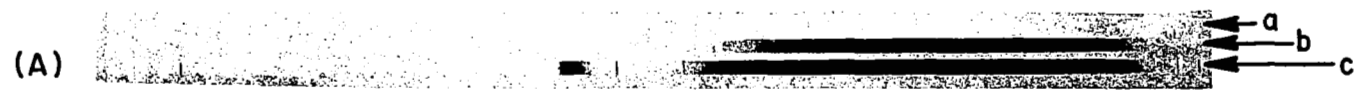


FIGURE 5

a = Toluene second Stokes only
b = Dye laser only

TABLE I
Representative Dye Lasers

Dye	Solvent ^(a)	Pumping Scheme ^(b) LPL, AFPL, LFPL	Stability of Dye Solution	Lasing Wavelength ^(c) and Color
7 Hydroxycoumarin	Water (buffered to pH=9)	AFPL	not stable	~4588Å, blue
fluorescein-Na Salt	ethanol	LPL, AFPL	stable	~5370Å, green
rhodamine 6G	ethanol	LPL, AFPL, LFPL	stable	~5800Å, yellow
rhodamine B	ethanol	LPL, AFPL	stable	~6100Å, red
cryptocyanine	glycerol	LPL	not stable	~7300Å, deep red
DTTC iodide ^(d)	DMSO	LPL	not stable	~8000Å, near I.R.
Dye 11 ^(e)	acetone	LPL	--	~10000Å, I.R.
rhodamine 6G	Stycast [®] epoxy	LPL	stable	~5550, yellow green
rhodamine B	Stycast [®] epoxy	LPL	stable	~5850, yellow
red fluorescing ^(f) plastic	Acrylic plastic	AFPL, LFPL	stable	~6340Å, red
yellow fluorescing ^(g) plastic	Acrylic plastic	AFPL, LFPL	stable	~6000Å, orange

- a. There may be several possible solvents
- b. LPL = Laser pumped lasing
AFPL = Annular Flashlamp pumped lasing
LFPL = Linear Flashlamp pumped lasing
- c. When flashlamp pumped lasing has been achieved the wavelength and color given are for this type of excitation. Also note that the particular wavelength can be adjusted by ~±50Å by adjustment of cavity Q and solution concentration.
- d. 3,3'-diethylthiatricarbocyanine iodide
- e. 11'-Diethyl 44'-quinotricarbocyanine iodide. Y. Miyzgoe and M. Maeda, Appl. Phys. L. 12, 206 (1968).
- f. Obtained from American Cyanamid Co.
- g. Obtained from Rohm and Haas Co.

Frequency- and Time-Dependent Gain Characteristics
of Laser- and Flashlamp-Pumped Dye Solution Lasers*

M. Bass, T. F. Deutsch and M. J. Weber

Raytheon Research Division

Waltham, Massachusetts

Abstract

Dye solution lasers are observed to lase at shorter wavelengths when laser-pumped than when flashlamp-excited. A comparison of the computed frequency- and time-dependent gains for the two pumping methods explains this behavior and the observed Q dependence of the lasing frequency. This treatment also suggests a new technique for frequency tuning dye lasers.

* The research reported in this paper was sponsored in part by the Electronics Research Center under NASA Contract NAS 12-635; to be published Appl. Phys. Lett. (August 15, 1968).

Visible laser action in solutions containing organic dye molecules has been achieved using both laser pumping⁽¹⁻³⁾ and short-pulse flashlamp pumping.⁽⁴⁻⁶⁾ A summary of lasing wavelengths observed by us and others for dye solutions which lased with both types of excitation is presented in Table I. Despite a variety of experimental conditions, the wavelengths obtained using laser pumping are always shorter than those obtained by flashlamp excitation. This behavior can be understood by comparing the gain characteristics of the lasing medium for each type of pumping. An extension of McCumber's approach⁽⁷⁾ to the treatment of phonon-terminated solid-state lasers is used. The frequency dependence of the gain and its evolution with time are computed using the time-dependent ground and excited state populations and the spontaneous emission spectrum. The calculations account for the observed lasing frequencies of rhodamine B, explain the reported⁽⁸⁾ Q dependence of the lasing frequency, and suggest a new technique for frequency tuning dye lasers.

Our laser-pumped data in Table I was obtained by focusing the second harmonic of a Q-switched ruby (3470Å) or Nd:YAG (5320Å) laser into a 2 cm long dye cell with a 12 cm focal length lens; the risetimes ranged from 10 - 30 nsec. Lasing parallel to the direction of the pump light was achieved by aligning the windows of the cell to form a cavity composed of two ~ 5 % reflectors. For flashlamp pumping, a cavity with broadband output coupling and losses estimated to be ~ 10% was used. Solutions of rhodamine 6G, fluorescein-Na salt, and acridine red in ethanol were excited by the coaxial flashlamp described previously;⁽⁶⁾ the lamp had a risetime of ~ 200 nsec and a discharge length of 15 cm. A similar lamp having a risetime of ~ 500 nsec was used to obtain the rhodamine B in methanol data analyzed below. The lowest fluorescein-Na salt and acridine red concentration for which laser-pumped lasing was achieved was 10^{-4} M. Note that if the wavelength difference in Table I for laser vs. flashlamp pumping was due only to the effect of increasing self-absorption with increasing concentration, as discussed elsewhere,^(1, 9) the laser pumped laser should have had the longer lasing wavelength. The unusually long wavelength observed by Schäfer et al. for laser-pumped rhodamine B⁽²⁾ arises from the concentration used, which was almost two orders of magnitude greater than ours.

TABLE I

SUMMARY OF LASING WAVELENGTHS FOR VARIOUS DYE SOLUTIONS

Dye	Solvent	Molar Concentration	Dye Laser Wavelength(Å)			Ref.
			Laser Pump 3470Å	Laser Pump 5320Å	Flashlamp Pump	
Rhodamine B	methanol	5×10^{-5}		5790	6170	a
	ethanol	5×10^{-5}		5790	6220	a
	"	-	5770	5770		b
	"	2×10^{-3}	6080			c
	polymethyl- methacrylate	6×10^{-5}			6250	d
Rhodamine 6G	ethanol	10^{-4}		5620	5950	a
	"	10^{-4}			5990(e)	a
	"	10^{-4}			5850	f
	"	-	5650	5650		b
	"	-	5520-(h) 5940			g
	polymethyl- methacrylate				6010	d
Acridine red	ethanol	10^{-4}		5840		a
	"	5×10^{-5}			6150	a
	"	10^{-4}			6015	f
	"	10^{-3}	orange			i
Fluorescein- Na Salt	ethanol	10^{-4}	5370			a
	"	5×10^{-5}			5600	a
	" , H ₂ O	10^{-4}			5500	f
	" "	10^{-3}	green			i
	H ₂ O		5350			b

a. Present work

b. Ref. 3

c. Ref. 2

d. Ref. 15

e. Obtained using a 170 J pulse from an FX-38 flashlamp; risetime 2 μ sec, duration 20 μ sec (FWHM)

f. Ref. 4

g. Ref. 13

h. Tuned with a grating in the cavity.

i. Ref. 1

The gain of organic dye solutions varies with both frequency and time during the pumping pulse. To analyze this dependence, we consider a system composed of two sets of energy levels corresponding to the ground and first excited singlet states and associated vibrational levels and having populations per unit volume of N_- and N_+ , respectively. The populations within each set are assumed to attain a thermal equilibrium distribution characteristic of the solution temperature T in a time short compared to the pumping time or singlet decay time. Decay to the triplet level system is neglected in the present calculations.⁽¹⁰⁾ Populating of and selective absorption from triplet levels can be significant, however,^(1, 11) and will be treated in detail elsewhere. McCumber⁽⁷⁾ has shown that for a system of two sets of energy levels, the gain at frequency $\sigma(\text{cm}^{-1})$ is given by

$$g(\sigma) = \{N_+ - N_- \exp [hc (\sigma - \sigma_0)/kT]\} f(\sigma)/n^2 \sigma^2, \quad (1)$$

where for dye solutions $f(\sigma)$ is the fluorescence intensity in photons per sec per unit frequency interval per unit solid angle for each emitting molecule, n is the refractive index, and $hc\sigma_0$ is the net free energy required to excite one molecule. For dyes having mirror-image absorption and emission spectra, σ_0 is taken to be the frequency of the 0-0 transition.

It is evident from Eq. (1) that the frequency at which the gain is a maximum, and thus the lasing frequency at threshold, is governed by the time-dependent populations and the emission spectral function $f(\sigma)$. The variation of the populations N_+ during the pumping pulse up to threshold can be found from the rate equation

$$\frac{dN_+}{dt} = - \left[\frac{1}{\tau} + P(t) \right] N_+ + NP(t), \quad (2)$$

where τ is the lifetime of the excited singlet state, $P(t)$ is the pumping rate and $N = N_+ + N_-$. Computer solutions of Eq. (2) were obtained using the measured time dependence and estimated intensities of $P(t)$. For laser pumping, a 10 mJ, 30 nsec pulse applied to a 5×10^{-5} M solution of rhodamine B in methanol, $\tau \approx 2$ nsec⁽¹²⁾, corresponds to a $[\tau P(t)]_{\text{max}} \sim 1$. Flashlamp pumping, in contrast, corresponds to the weak

pumping limit $[\tau P(t)]_{\max} \ll 1$. Because the spectral output and electrical-to-optical conversion efficiency of the flashlamp was not well established, estimates of $\tau P(t)$ were uncertain and therefore calculations were made using a range of τP values (the final choice being guided by the observed laser frequency and time at threshold). The $N_+(t)$ values for both laser and flashlamp pumping together with the measured $f(\sigma)$ for rhodamine B in methanol were substituted into Eq. (1); the resulting gain vs. frequency curves at various times during the excitation pulse are shown in Fig. 1. For laser pumping, oscillation began at about 5 nsec and at a frequency of $17,260 \text{ cm}^{-1}$. The estimated gain required for oscillation in the cavity used was $\sim 1.5 \text{ cm}^{-1}$. From Fig. 1a, this gain value is first reached at ≈ 4.8 nsec and at a frequency of $\approx 17,250 \text{ cm}^{-1}$, in good agreement with experiment. Similarly, for flashlamp pumping ($\approx 20\text{j}$ electrical input energy) oscillation began at ≈ 200 nsec with a frequency of $16,200 \text{ cm}^{-1}$. This behavior is again predicted by Fig. 1 based upon a required threshold gain of $\sim 3.5 \times 10^{-3} \text{ cm}^{-1}$.

An examination of Fig. 1 reveals why dye solutions lase at different frequencies for the different pumping and cavity configurations. Whereas with flashlamp excitation there is never any gain at frequencies greater than $\sim 17,000 \text{ cm}^{-1}$, with laser excitation the gain is a maximum at frequencies as high as $\sim 17,600 \text{ cm}^{-1}$. Since the end-pumped, laser-excited dye cavity requires high gain to achieve oscillation, the lasing frequencies are higher than in the flashlamp-pumped case. It should be recognized that for a given cavity, if the pumping energy and risetime of the flashlamp were sufficient to produce the same inversion as the laser pump, the same $g(\sigma)$ curve and lasing frequency would be obtained. However, the time of threshold may be different because it is dependent upon the time development of the pump pulse. More typically, though, the gains achievable with laser pumping are much greater than those for existing flashlamp pumping.

Fig. 1 also demonstrates that for a given excitation pulse, the gain and the frequency at which it is a maximum depend upon the time interval following the initiation of pumping. This is shown explicitly in Fig. 2

where these quantities are plotted as a function of time for the flashlamp case. Clearly the lasing frequency can be selected by introducing a Q switch into the dye laser cavity and opening it after the appropriate time interval. In addition, since the gain depends on this time interval too, it should be possible to adjust the time of opening the Q switch so as to optimize the laser output.

Schäfer et al. ⁽⁸⁾ observed that the emission wavelength of a dye laser increased or decreased with increasing or decreasing cavity Q. The behavior is immediately understandable from inspection of Fig. 1 and suggests that frequency selection can be obtained by careful choice of cavity Q. This is a dynamic process in that the time interval between initiating pumping and the start of laser oscillation also depends upon the cavity Q and increases with decreasing Q. For a fixed Q, the greater the pumping rate, the earlier oscillation begins; however, the frequency remains the same. We have observed this effect for flashlamp-pumped rhodamine B. With flashlamp pumping of a 10^{-4} M solution of rhodamine B in methanol, an increase in the input energy to the flashlamp by a factor of 1.3 resulted in a decrease in the interval before lasing began by a factor of 1.3. The lasing wavelength remained the same.

Soffer and McFarland, using rhodamine 6G in ethanol, have shown that a dye laser can be tuned over more than 400 \AA by inserting a wavelength selecting element, such as a grating or a filter, into the laser cavity. ^(13, 14) Their work indicated further that laser-pumped rhodamine 6G had gain in the spectral region where we observed it to lase with flashlamp pumping. It is readily apparent from the calculated gain curves in Fig. 1a for laser pumping that the same should be true for rhodamine B in methanol. To verify this, the lasing wavelengths of several solutions were measured when various glass filters were inserted into the dye laser cavity. The cavity was formed by an external 98.5% R broadband mirror and the $\sim 5\%$ reflectance of one window of the dye cell. The introduction of the filter into the cavity makes the gain required for laser oscillation high where the filter

absorbs and low where it transmits; thus lasing will occur at the latter wavelengths. The results, summarized in Fig. 3, show that the lasing wavelength for laser-pumped rhodamine B can indeed be shifted to the red by over 300\AA in agreement with the range predicted in Fig. 1. The effect of a wavelength selecting element in the laser cavity on the frequency-dependent gain curves can be predicted by the addition of an appropriate multiplicative factor in the gain expression, Eq. (1).

We would like to thank Miss Winifred Doherty for programming the calculation and D. Woodward for experimental assistance. We thank H. Furumoto for useful discussions.

References

1. P. P. Sorokin, J. R. Lankard, E. C. Hammond, and V. L. Moruzzi, IBM J. of Res. and Dev. 11, 139 (1967) and addendum.
2. F. P. Schäfer, W. Schmidt, and K. Marth, Phys. Letters 24A, 280 (1967).
3. B. B. McFarland, Appl. Phys. Letters 10, 208 (1967).
4. P. P. Sorokin and J. R. Lankard, IBM J. of Res. and Dev. 11, 148, 1967.
5. B. B. Snavely, O. G. Peterson and R. F. Reithel, Appl. Phys. Letters 11, 275 (1967).
6. T. F. Deutsch, M. Bass, P. Meyer and S. Protopapa, Appl. Phys. Letters 11, 379 (1967).
7. D. E. McCumber, Physical Review 134, A299 (1964).
8. F. P. Schäfer, W. Schmidt, and J. Volze, Appl. Phys. Letters 9, 306 (1966).
9. M. Bass and J. I. Steinfeld, IEEE J. of Quantum Electronics QE-4, 53 (1968).
10. B. B. Snavely and A. V. Buettner (private communication) have measured triplet-triplet absorption for rhodamine B in methanol and find the peak at 6225Å . Although a population buildup in the lowest triplet level would be unimportant for the laser-pumped case, a significant accumulation may occur during flashlamp pumping, thus leading to an additional loss at 6225Å and pursuant modification of the gain curve in Fig. 1b.
11. P. P. Sorokin, J. R. Lankard, V. L. Moruzzi and E. C. Hammond, (to be published) J. Chem. Phys.
12. B. B. Snavely, Private Communication.

References (contd.)

13. B. H. Soffer and B. B. McFarland, Appl. Phys. Letters 10, 266 (1967).
14. B. H. Soffer, R. C. Pastor, H. Kimura, J. Linn and B. B. McFarland, Spectral Properties of Passively Q Spoiled Lasers, Semi Annual Technical Summary Report 30 Oct. 1967, Contract Nonr-5150 (00), ARPA Order Number 306.
15. O. G. Peterson and B. B. Snavely, Appl. Phys. Letters 12, 238 (1968).

Figure Captions

- Fig. 1 Calculated frequency - dependent gain of 5×10^{-5} M rhodamine B in methanol at various times (nsec) after pumping begins: (a) laser pumping, (b) flashlamp pumping. The time dependence and estimated intensity of the excitation pulses used in the calculations are shown in the inserts. Arrows indicate the observed lasing frequencies.
- Fig. 2 Calculated frequency at which the gain is a maximum (solid curve) and the maximum gain value (dashed curve) for 5×10^{-5} M rhodamine B as a function of time for flashlamp pumping.
- Fig. 3 Lasing wavelength as a function of concentration and with different Corning glass filters in the laser cavity for laser-pumped rhodamine B solutions.

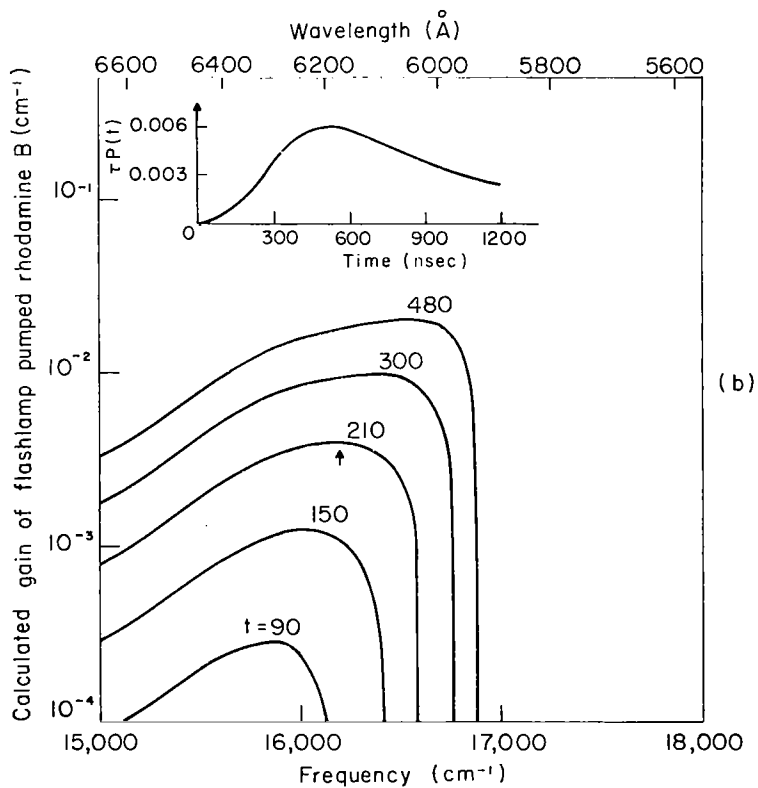
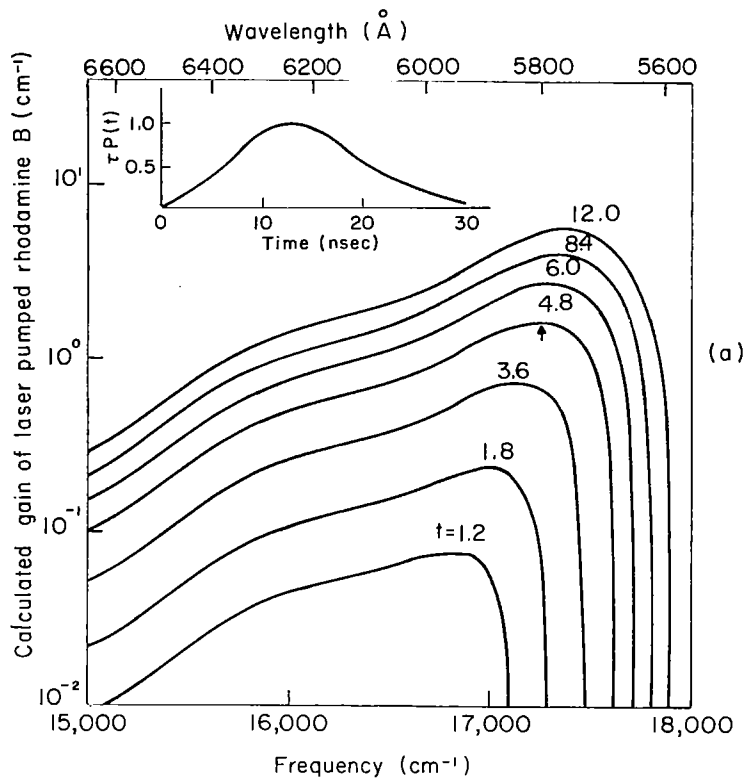


FIGURE I

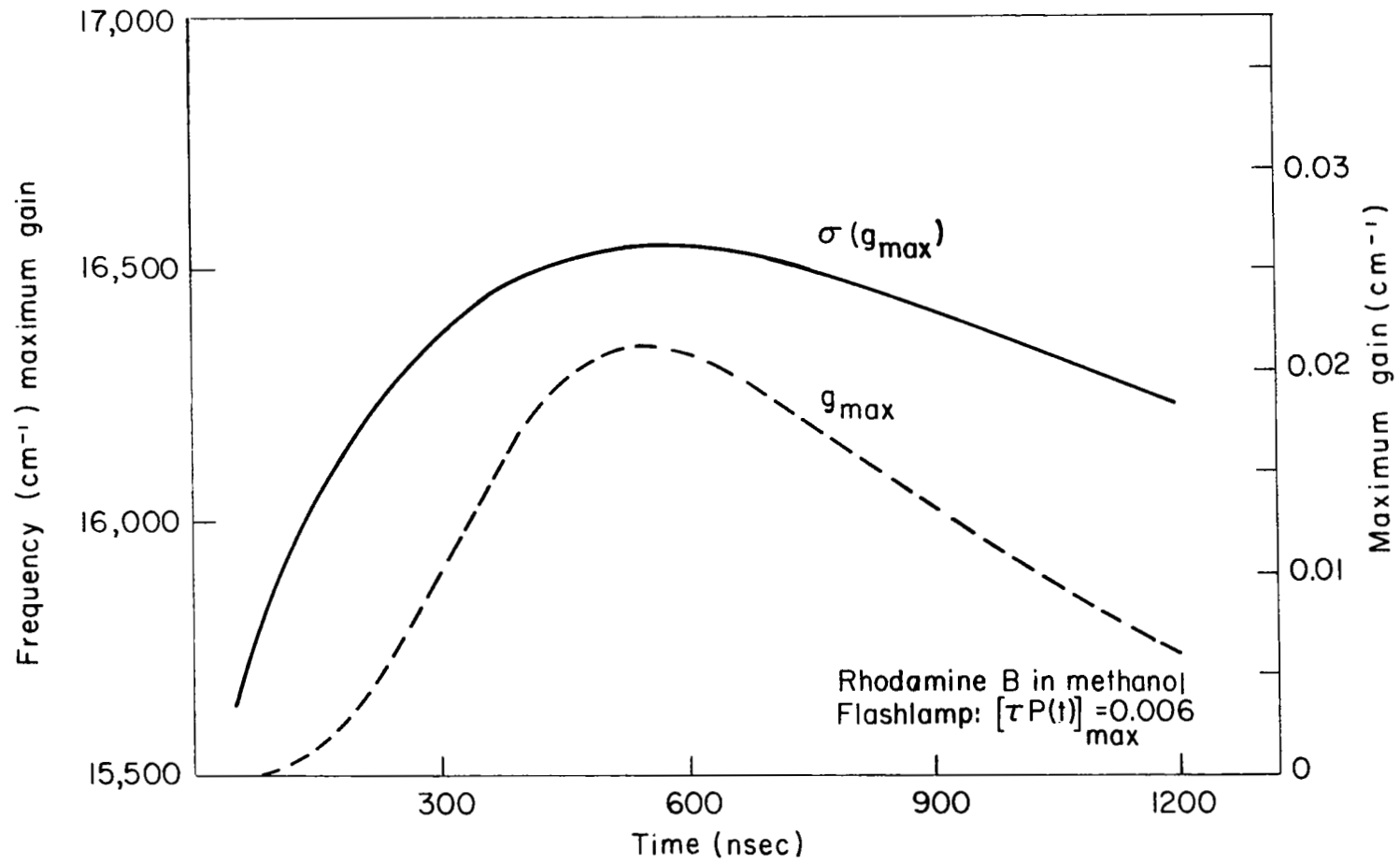


FIGURE 2

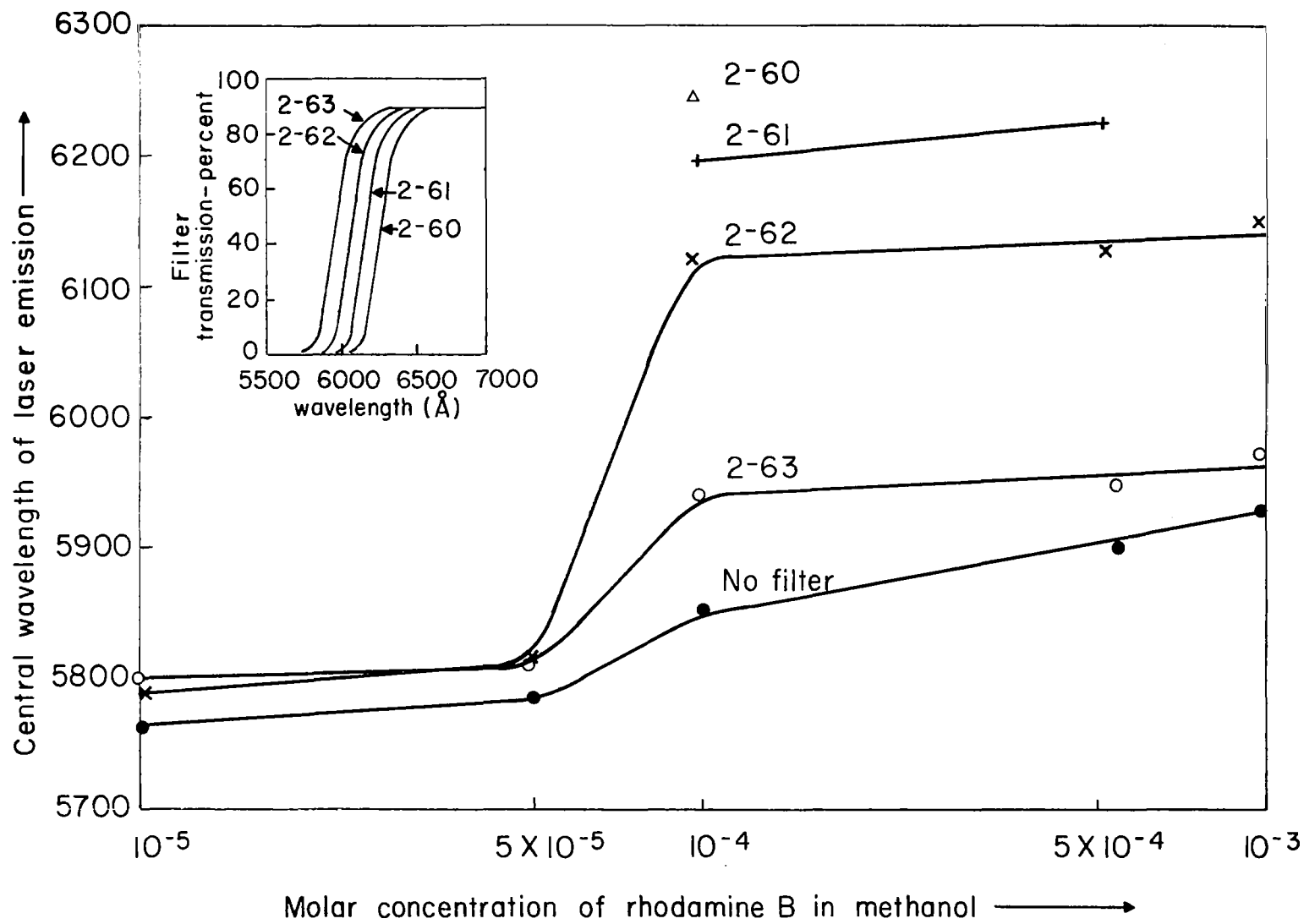


FIGURE 3